Journal of Natural Fibers

ISSN: 1544-0478 (Print) 1544-046X (Online) Journal homepage: www.tandfonline.com/journals/wjnf20

Hybrid Reinforcement of Traditional Bricks Using *Opuntia ficus-indica cactus* Fibers and Biochar: Optimization and Prediction via RSM and ANN

Hocine Boudjehm , Messaouda Boumaaza, Ahmed Belaadi , Wail Harasani , Mostefa Bourchak , Ibrahim M. H. Alshaikh & Djamel Ghernaout

To cite this article: Hocine Boudjehm , Messaouda Boumaaza, Ahmed Belaadi , Wail Harasani , Mostefa Bourchak , Ibrahim M. H. Alshaikh & Djamel Ghernaout (2026) Hybrid Reinforcement of Traditional Bricks Using *Opuntia ficus-indica cactus* Fibers and Biochar: Optimization and Prediction via RSM and ANN, Journal of Natural Fibers, 23:1, 2661856, DOI: 10.1080/15440478.2026.2661856

To link to this article: https://doi.org/10.1080/15440478.2026.2661856

Published online: 23 Apr 2026.

JOURNAL OF NATURAL FIBERS
2026, VOL. 23, NO. 1, 2661856
https://doi.org/10.1080/15440478.2026.2661856

Hybrid Reinforcement of Traditional Bricks Using *Opuntia ficus-indica cactus* Fibers and Biochar: Optimization and Prediction via RSM and ANN

Hocine Boudjehm[a], Messaouda Boumaaza[b], Ahmed Belaadi[c], Wail Harasani[d], Mostefa Bourchak[d], Ibrahim M. H. Alshaikh[e], and Djamel Ghernaout[f]

[a]Department of Architecture, Faculty of Science and Technology, University 8 Mai 1945 Guelma, Guelma, Algeria; [b]Laboratory of Civil Engineering and Hydraulics (LGCH), University 8 Mai 1945 Guelma, Guelma, Algeria; [c]Department of Mechanical Engineering, Faculty of Technology, University 20 Août 1955-Skikda, Skikda, Algeria; [d]Aerospace Engineering Department, King Abdulaziz University, Jeddah, Saudi Arabia; [e]Civil Engineering Department, Faculty of Engineering, University of Science and Technology (USTY), Sana'a, Yemen; [f]Chemical Engineering Department, College of Engineering, University of Ha'il, Ha'il, Saudi Arabia

ABSTRACT

To address the pressing housing demand brought on by issues with population increase, earth construction materials with good mechanical and thermal qualities must be developed. To meet this objective, earth bricks were reinforced with a hybrid blend of Opuntia ficus-indica cactus plant (OFICP) fibers and biochar obtained through the pyrolysis of the same plant. The fibers, incorporated at 0.5% and 1% by weight, underwent alkaline treatment using sodium bicarbonate ($NaHCO_3$) at concentrations of 5%, 7%, and 10%, with immersion durations of 24, 72, and 168 hours. The multiple nonlinear regression models RSM et ANN were generated utilizing variables such fiber content, immersion time, and NaHCO3 content in order to predict compressive and flexural strength as well as thermal conductivity. According to the findings, 0.5% fibers treated with 7% NaHCO3 for 72 hours constituted the ideal formulation. The mix's workability was much improved by the addition of biochar. However, these mechanical characteristics gradually decreased as the fiber content increased above this level. Thermal conductivity dropped from 0.64 W/m·K in specimens without OFICP fibers to 0.37 W/m·K in those with 1% OFICP and biochar, demonstrating a significant decrease in heat transmission as a result of fiber inclusion and an improvement in thermal insulation.

HIGHLIGHTS

- The addition of *Opuntia ficus-indica cactus* and biochar to adobe bricks optimally improves their mechanical strength.
- The addition of *Opuntia ficus-indica cactus* and biochar enhances the thermal insulation of adobe bricks.
- This composite offers promising potential applications in thermal insulation materials.
- The development of models for estimating flexural strength, compressive strength and thermal conductivity is described.

摘要

為解決人口增長所引發的迫切住房需求，必須開發兼具優良機械性能與熱性能的土質建築材料。為達成此目標，本研究採用仙人掌 (Opuntia ficus-indica，簡稱OFICP)纖維與該植物熱解所得的生物炭所製成的混合物，對土磚進行加固。將重量比為0.5%及1%的纖維，分別以5%、7%及10%濃度的碳酸氫鈉 ($NaHCO_3$)進行鹼處理，浸泡時間分別為24、72及168小時。研究利用纖維含量、浸泡時間及$NaHCO_3$濃度等變數，建立多重非線性回歸模型 (RSM)與人工神經網路 (ANN)，以預測其抗壓強度、彎曲強度及熱導率。根據研究結果，含0.5%纖維並以7% $NaHCO_3$處理72小時的配方，被認定為最佳配方。添加生物炭後，混合物的可塑性顯著提升。然而，當纖維含量超過此水平時，這些力學特性便逐漸下降。熱導率從不含 OFICP 纖維的試樣中的 0.64 W/m•K，降至含 1% OFICP 纖維與生物炭試樣中的 0.37 W/m•K，顯示出因添加纖維而導致的熱傳導顯著降低，以及隔熱性能的提升。一項優化研究指出，含有 0.4% (重量比)經 83 小時 8% $NaHCO_3$ 處理之 OFICP 纖維的穩定土磚 (SEBs)，具備最佳的熱學與機械性能。由此製成的黏土磚將有助於全球興建經濟實惠且永續的建築，特別是在資源有限的地區作為砌體磚使用。

KEYWORDS

Opuntia ficus-indica cactus plant; *cactus* fibers; earthen blocks; thermal conductivity; mechanical characteristics; optimization

關鍵詞

仙人掌; 仙人掌纖維; 土磚; 熱導率; 機械特性; 優化

CONTACT Ibrahim M. H. Alshaikh ibrahimalshaikh86@gmail.com Civil Engineering Department, Faculty of Engineering, University of Science and Technology (USTY), Sana'a, Yemen

Introduction

Currently, eco-construction research focuses on recovering local materials like earth, volcanic ash, and industrial waste while enhancing their technological properties with the addition of Portland cement, lime, activated binder, and natural fibers. Stabilizing compressed earth blocks (CEBs) using activated binder or geopolymer binder and Portland cement have been found to be a potential alternative for ecologically friendly building in numerous investigations on the economic importance of local natural resources in building (Dime et al. 2022; Ghadir and Ranjbar 2018; Oti and Kinuthia 2020). These days, compressed and stabilized earthen blocks (CSEB) blocks are becoming an area of ecological conservation interest, cultural asset prevention, and heritage restoration.

Adobes, however, have comparatively low flexural and compressive strengths (Serebe et al. 2024). Depending on the size and type of raw materials utilized, their compressive strengths range from 0.6 to 6.6 MPa (Ashour et al. 2015). Many techniques have been employed to increase their mechanical strength, including the inclusion of natural fibers (Bamogo et al. 2020; Boumaaza et al. 2022; Gueffaf et al. 2025), or cement-based mineral stabilization (Medjelekh et al. 2016). Although cement stabilization is frequently superior, most studies do not recommend this method since cement manufacturing is costly, energy-intensive, and harmful (Gavali et al. 2019; Maaze and Shrivastava 2023). Several studies have shown that adding fiber to the clay matrix lowers heat conductivity (Chihab, Laaroussi, and Garoum 2023; Dao et al. 2018; Omrani et al. 2020; Rashid et al. 2019). Furthermore, an examination of numerous research on the impact of adding fiber to adobe often yields improvements in compressive and flexural strengths up to a specific content, after which the strength values decrease. A study by Humphrey Danso et al. (2015a) links the fiber aspect ratio of different natural fibers to the strength (compression, tension) of blocks (Ige and Danso 2021). This ideal fiber content varies depending on the earth's properties and the methods used to produce adobe.

Numerous research on date palm fiber reinforcement in CSEB blocks demonstrate that while date palm fiber reinforcement offers acceptable durability features, the block's compression and tensile strengths diminish when the fiber content rises above 0.5% (Abdeldjebar et al. 2018; Taallah and Guettala 2016). Millogo et al. (2014) investigated pressed earth blocks reinforced with 3 cm and 6 cm kenaf fibers. For size 3 cm and size 6 cm, respectively, the ideal values for increasing compressive strength were 0.3 and roughly 0.5 weight percent. the ideal values for increasing compressive strength were 0.3 and roughly 0.5 weight percent for size 3 cm and size 6 cm, respectively.

According to Zardari, Lakho, and Amur (2020), the addition of jute fibers (0.5–2%) causes voids related to water removal during drying, which lowers the compressive strength of CEBs (from 3.7 to 2.4 MPa). Conversely, tensile strength (0.5–1%) rises little (from 0.69 to 0.74 MPa. According to other research (Salih, Osofero, and Imbabi 2020), adding sugar cane bagasse (5%) and chicken feather fibers (7%), with an ideal length of 15 mm, greatly increases mechanical strength. A substantial improvement in performance using maize silk fibers (0.25–0.5%), reaching +177% in compression and +88% in traction (Tran, Satomi, and Takahashi 2018).

The bonding qualities and features of natural fibers may be improved via treatments. The high mechanical bonding procedures used in these investigations have an impact on the unfired earthen blocks' tensile and compressive strengths. Fewer studies treat the material before adding it to the earthen mixture (Gavali et al. 2019; Jesudass et al. 2021; Poinot et al. 2018). Future research is advised to use the fiber treatments to enhance the efficiency of uncooked earth blocks. The impact of raw and alkali-treated date palm fibers on the characteristics of compressed earth blocks (CEBs) was investigated by Taallah and Guettala (2016). Compared to CEBs without fibers, the insertion of fibers raises capillary uptake while decreasing apparent density. For raw fibers, the water uptake coefficient ranges from 4.53% to 5.26%, while for treated fibers, it ranges from 4.65% to 5.69%. Immersion or capillarity measurements of water absorption rise as fiber content does. In comparison with fiberless blocks, the compressive strength increased by 3.9% when the fiber was treated with 0.05% alkali. According to the authors (Taallah and Guettala 2016), alkali-treated fibers have a higher strength value than untreated fiber blocks. The significance of alkaline treatment of palm fibers in enhancing the properties of compressed earth bricks (CEB) stabilized with alkaline binders was illustrated by Kamwa et al. (2025). Their research shows that adding soda-treated fibers (NaOH) at varying lengths (4 and 16 cm) and concentrations (0.1 to 0.5% by mass) improves mechanical performance, increases matrix-fiber adhesion, and decreases water absorption. CEBs reinforced with 0.4% treated fibers.

The durability features of CSEB are significantly improved by the texture and characteristics of date palm fiber (Abdeldjebar et al. 2018; Taallah et al. 2014). When reinforced with CSEB block, the coconut fiber exhibits good wearing strength (Danso et al. 2015b). The date palm fiber's heat conductivity and water absorption were investigated by Taallah and Guettala (2016). When date palm fibers were introduced, the block's capillary absorption increased. At the same time, it was revealed that as fiber content raised, heat conductivity decreased. Water uptake for all different fiber content reinforcements was found to be within allowable bounds. Jute fibers appear to improve the behavior of composite materials in compression during freezing-thawing cycles (Laborel-Préneron et al. 2016).

The use of plant-based materials as mechanical reinforcement – particularly Opuntia ficus-indica cactus fibers – is supported by numerous scientific findings. These fibers are abundant, easily accessible, and their physico-chemical, microstructural, and mechanical properties are well documented, making them promising candidates for sustainable construction applications.

However, despite growing interest in natural additives, research to examine *Opuntia Ficus Indica's* role in soil stabilization remains limited. In particular, the influences of fiber concentration and curing duration on the mechanical performance of fiber-reinforced earth materials have not been extensively explored. One notable exception is the study by Aparicio et al. (2019), which investigated the use of cactus mucilage as a binder in mud blocks. That work yielded promising results, including reduced water absorption and improved compressive strength, highlighting the potential of this plant in enhancing earthen construction materials. The study showed encouraging outcomes in relation to decreased water absorption and compressive strength. In this context, the current study focuses on using biochar and discarded *Opuntia ficus-indica* fibers to stabilize the soil. It examines the effects of fiber content, immersion duration, and $NaHCO_3$ concentration on the bricks' mechanical and thermal characteristics. The relationship between compressive and tensile strength is established using experimental data. Additionally, predictive models for thermal conductivity, flexural strength, and compressive strength are suggested.

Recently, techniques such as artificial neural networks (ANN) and response surface methodology (RSM) have been applied to optimize the properties of bio-based materials with biochar (Alioui et al. 2026; Baibordy, Yekrangnia, and Jahromi 2025; Ganasen et al. 2024; Limami et al. 2023; Tan et al. 2026). Nakkeeran et al. (2024) combined ANN/RSM/TOPSIS for Bio-Bricks (peanut shells), obtaining $R^2 > 0.99$ in prediction. Mebarkia et al. (2025a) identified 30% CKD furnace dust at 800–896°C as optimal for low-temperature clay bricks. The relationships between formulation parameters (OFICP fiber content, $NaHCO_3$ concentration, immersion time) and mechanical and thermal properties are inherently non-linear due to complex fiber–matrix interactions, biochar-induced porosity and the synergistic effects of alkaline treatment. Analytical models or simple linear regressions are insufficient to capture these non-linearities, as demonstrated in recent studies on earthy materials. The application of RSM and ANN techniques to forecast mechanical and thermophysical characteristics in bricks containing *Opuntia ficus-indica* fibers and biochar has not been studied before, making this study unique, which constitutes the methodological novelty of this study. The hybrid RSM-ANN approach adopted here, supported by robust validation (cross-experimental tests, $R^2 > 0.95$), enables accurate prediction, effective multi-objective optimization, and increased transferability of results to other sustainable formulations.

Materials and methods

Materials used in this study

Opuntia Ficus-indica cactus plant or the prickly pear is a succulent plant of the *Cactaceae* family that grows widely in semi-arid and arid regions, especially in the Mediterranean basin. It is characterized by its fleshy cladodes, or flattened stems, which are rich in cellulose fibers, mucilage, and bioactive substances and are resistant to harsh climates. This species is gaining attention in the realm of bio-based and sustainable materials in addition to its traditional usage in food and medicine. OFICP fibers were gathered for this study in the Guelma region of north-eastern Algeria (36°27′N, 7°25′E), which has a semi-arid climate that is favorable cactus to the plant's growth (Figure 1). After being manually picked and allowed to dry outdoors, the adult cladodes were processed to extract the fibers needed to make stabilizing earth bricks.

To improve the mechanical qualities of the compacted earth blocks, several treatments were applied to the OFICP fibers to be utilized as reinforcement for SEB prior to cutting. In this case, OFICP fibers will be immersed for 24, 72, and 168 h in sodium bicarbonate ($NaHCO_3$) at concentrations of 5%, 7%, and 10%. Following each treatment, the OFICP fibers were thoroughly submerged in water, drained in distilled water for half an hour, and then meticulously cleaned to get rid of any remaining organic matter and contaminants. Finally, the resultant OFICP fibers were dried at room temperature in the shade until their masses stabilized. After being processed, the OFICP fibers were chopped into 10 to 15 mm pieces to be used as reinforcement in the various SEB formulations.

The biochar used in this research was produced through the pyrolysis of *Opuntia ficus-indica* cactus fibers, a process involving thermal decomposition of biomass in an oxygen-limited environment. The fibers were pyrolyzed for 30 min at 500°C in a sealed furnace with a venting device to discharge volatile organic chemicals. The cactus biomass was converted by this heat treatment into a stable, carbon-rich substance with a microporous structure that could retain carbon over time. To guarantee uniform dispersion inside the earth matrix, the produced biochar was crushed into fine particles after cooling in an airtight container. The soil used in the experimental program was sourced from a deposit adjacent to a brickyard and highway construction site near Guelma. This locality is traditionally known for adobe brick production, widely practiced by local communities engaged in sustainable building techniques. Grain size analysis was performed in compliance with the NF P 18–560 standard (1990) to determine the granular content of the soil (Figure 2). The soil's suitability for earthen construction is confirmed by the particle size distribution curve, which falls completely within the recommended zone specified by standard XP P 13–901 for CEBs (2017). The soil used has a particle size distribution of 5% clay (particles < 0.002 mm), 15% silt (0.002–-0.063 mm), 50% sand (0.063–2 mm) and 30% gravel (>2 mm). The biochar contains 10% fines (<0.063 mm) and 90% fine sand, ensuring excellent particle size complementarity with the earth matrix to optimize compaction, limit shrinkage/cracking and improve the mechanical and capillary performance of SEB bricks. A relatively compact structure with balanced porosity was indicated by the soil's specific density of 2615 kg/m^3 and apparent density of about 1180 kg/m^3. The soil was categorized as moderately plastic by the Atterberg limits, which showed a liquid limit (LL) of 34% and a plasticity index (PI) of 15%. This characteristic is beneficial for shape, compaction, and dimensional stability during drying and curing. Concurrently, a finer particle size distribution is seen in the biochar. This suggests that when added to soil mixtures, it may enhance matrix homogeneity and fill interstitial spaces.

Bricks fabrication

Adobe bricks are produced by mixing clay, fibers from the *Opuntia ficus-indica* cactus, biochar and water. Brick samples manufactured with OFICP percentages of 0.5 and 1% treated with 5, 7, and 10% $NaHCO_3$% for 24, 72, and 168 h with1% biochar. After blending the dry components 30 min for sufficient plasticity, the

Figure 1. Tissue of *Opuntia ficus-indica* cactus fibers (OFICP).

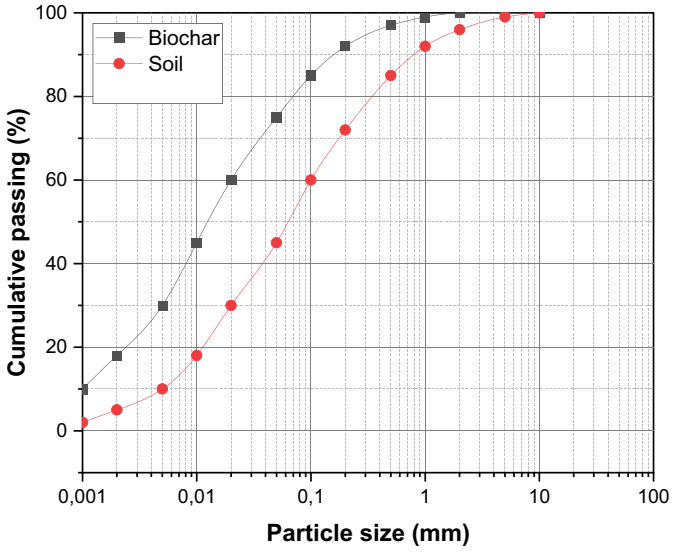

Figure 2. Soil and biochar particle size distributions.

mixtures were hydrated to achieve the necessary texture. This is created by pyrolyzing OFICP waste at 500°C, which transforms plant remnants into a porous carbonaceous substance that has the potential to store CO_2 indefinitely. According to the experimental plan, bricks composed of biochar and OFICP fibers were produced (Table 1). Eighteen distinct brick compositions with varying fiber percentage, immersion time, and $NaHCO_3$ concentration were created. The development of eco-friendly building materials that are tailored to local climate restrictions has a bright future because of this plentiful and renewable natural resource.

Static pressing is the compaction technique suggested from the Center for Development of Enterprise (CDE 2000). To remove moisture, the soil is first oven-dried for 24 h at 105°C. For unreinforced specimens, mixtures were made with 8% water and a consistent dry soil percentage of 92%. The additive mass was deducted from the soil fraction for OFICP enhanced formulations while keeping the water content constant. The mixture was manually mixed with dry OFICP and humidified before being put into molds that had been lightly lubricated and compressed at 17.5 MPa using a hydraulic press. The specimens were demolded right away and kept at 23 ± 2°C and 34 ± 3% relative humidity until they were tested 28 days later. Table 1 lists the many SEB formulations that were produced along with their nomenclature. The experimental protocol for manufacturing stabilized bricks is illustrated in Figure 3.

Tests conducted

After 28 days of curing, three-point bending tests are performed on specimens with dimensions of 40 × 40 × 160 mm^3. These experiments were carried out at a displacement control speed of 3 mm/min. According to the (2000) standard, the bending strength (FS) for each SEB formulation is determined by averaging the values from six tests, the flexural strength (FS) for each formulation was determined by averaging the results of six separate tests. The same SEB formulations were then assessed under axial loading using unconfined compressive strength tests (CS), which were performed with the (2000) procedure.

Capillary water absorption is determined using the technique outlined in AFNOR standard XP P 13–901 (2017). The strategy is to submerge the facing surface for 10 min in a thin layer of water (5 mm) and track

Table 1. The level and design of the various process test parameters.

			Levels		
Factor	Unit	Symbol	Min (−1)	Medium (0)	Max (+1)
OFICP content	%	A	0.5	–	1
$NaHCO_3$ percentage	%	B	5	7	10
Duration	Hour	C	24	72	168

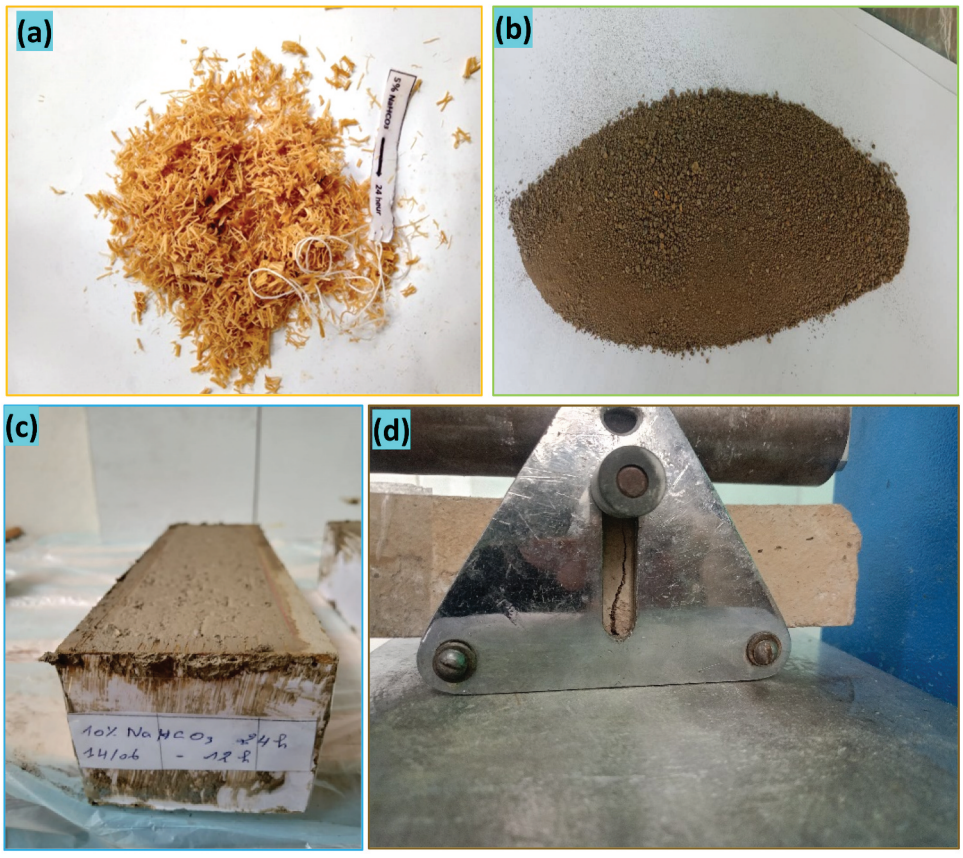

Figure 3. Experimental protocol for the production of SEBs specimens. a) short cactus fibers used b) earth soil c) mould filling d) compression test on cured SEB specimen.

the brick's mass absorption in this experiment. Equation 1 is used to determine the water uptake coefficient from this experiment:

$$CA = \frac{100(M_2 - M_1)}{S\sqrt{t}} \tag{1}$$

where CA represents the capillary rise resistance coefficient, M_2 (g) represents the block's weight following soaking in water, M_1 (g) represents the block's weight before to soaking in water, S (cm^2) represents the block's-soaked surface, and t (min) is the block's duration of immersion (min).

The European standard (2008) defines the slab test procedure for determining a brick's heat conductivity (TC). The TC of a material was measured using a flatbed thermal conductivity meter with two cooling units on either end of the heated central component. In order to ensure steady thermal transfer, the two specimens were placed in the spaces inside the heating and cooling systems (Eq. (2)).

$$\lambda = \frac{Q \text{ x } d}{2 \text{ x S x}(T_1 - T_2)} \tag{2}$$

The thermal capacity of the cooling system is denoted by Q (W), the test specimen's width by d (m), the thermal transfer region by S (m^2), and the temperatures of both the heating and cooling units by T_2 and T_1 (K).

Figure 4 shows a flowchart that illustrates the work process and describes the major phases of the study, from data collection to final analysis.

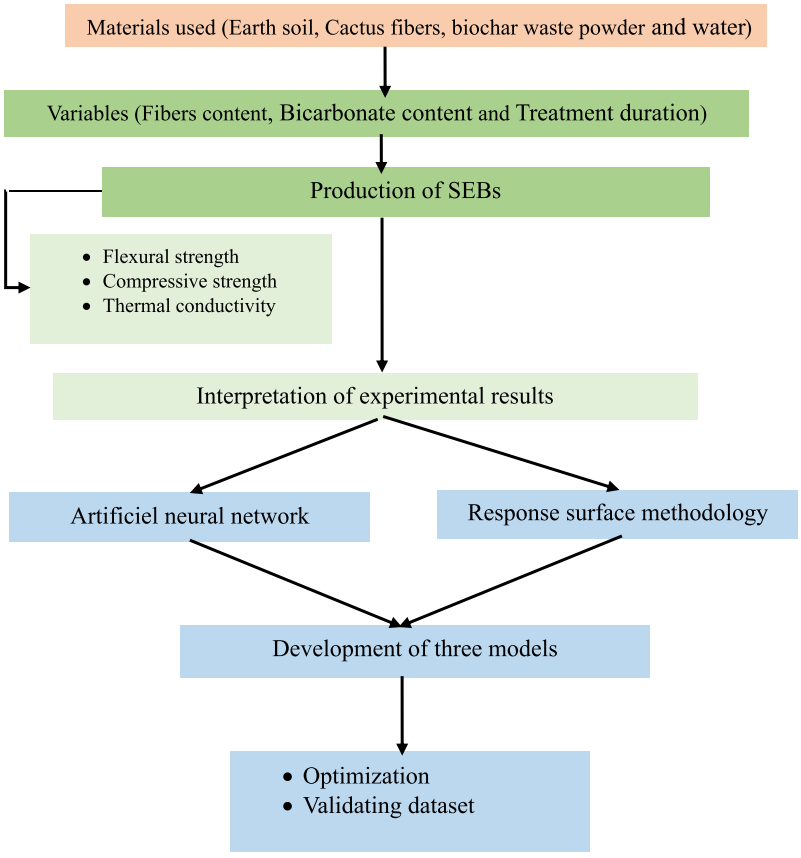

Figure 4. Research organization chart.

Mathematical models

Experiment plan using response surface methodology

RSM is a collection of mathematical and statistical methods designed to identify the present links between the independent parameters and the outcomes (Boumaaza et al. 2024; L. Li et al. 2022; Sinkhonde et al. 2021). The central composite design (CCD) was utilized using the Design Expert 13 software to process different data about bricks reinforced with biochar and OFICP fibers. The response surface approach considers three independent factors: OFICP% (A), $NaHCO_3$% (B), and immersion duration (C) as shown in Table 1.

The maximum and minimum amounts assigned to the centered components are represented by the codes (−1) and (+1), which are used to signify the different degrees utilized in the design of experiments (DOE) when adopting this methodology. To supply the process conditions created utilizing the RSM/CCD technique, 18 tests were carried out (Tables 2 and 3). Based on the independent characteristics, the compressive stress, flexural stress, and heat conductivity were calculated using a second-order polynomial equation (Eq (3)).

$$Y = \beta_0 + \sum_{1}^{k} \beta_i X_i + \sum_{1}^{k} \beta_{ij} X_i X_j + \sum_{1}^{k} \beta_{ii} X_i^2 \tag{3}$$

In this case, Y stands for the experiment's result (FS, CS, and TC), Xi and Xj for the independent parameters, β_{ij} and β_{ii} for the interaction impacts and quadratic coefficients, respectively, β_i and β_0 for the linear and fixed coefficients associated with the CCD estimation.

Artificial neural network

ANN modeling is a useful technique for reconstructing any kind of nonlinear processing's behavior (Chai, Eisenbart, Nikzad, Fox, Blythe, Blanchard, et al. 2023; Ofuyatan et al. 2022). Artificial neural networks

Table 2. Capillary absorption, heat conductivity, compressive strength, and bending strength values for bricks.

Mixture	Factors			Responses			
Runs	*A-OFICP (%)*	*B-NaHCO$_3$ T (°C)*	C-Duration (Hour)	Flexural strength (MPa)	Compressive strength (MPa)	Capillary absorption (g/cm^{2}min$^{0.5}$)	Thermal conductivity *(W/m.K)*
1	0,5	5	24	0.56 ± 0.09	3.42 ± 0.06	8.23 ± 0.03	0.581 ± 0.05
2	0,5	5	72	0.72 ± 0.05	3.52 ± 0.09	8.44 ± 0.06	0.571 ± 0.04
3	0,5	5	168	0.42 ± 0.09	3.31 ± 0.05	8.73 ± 0.05	0.563 ± 0.03
4	0,5	7	24	0.63 ± 0.07	3.48 ± 0.04	9.14 ± 0.03	0.551 ± 0.05
5	0,5	7	72	0.79 ± 0.08	3.57 ± 0.07	9.76 ± 0.06	0.531 ± 0.04
6	0,5	7	168	0.43 ± 0.05	3.36 ± 0.11	10.72 ± 0.05	0.511 ± 0.07
7	0,5	10	24	0.42 ± 0.06	3.34 ± 0.05	11.12 ± 0.02	0.461 ± 0.03
8	0,5	10	72	0.64 ± 0.18	3.43 ± 0.06	13.12 ± 0.04	0.421 ± 0.02
9	1	10	168	0.23 ± 0.11	3.19 ± 0.04	15.42 ± 0.03	0.401 ± 0.04
10	1	5	24	0.33 ± 0.06	3.29 ± 0.02	9.35 ± 0.03	0.399 ± 0.06
11	1	5	72	0.44 ± 0.04	3.32 ± 0.03	10.12 ± 0.04	0.396 ± 0.03
12	1	5	168	0.25 ± 0.05	3.23 ± 0.06	11.34 ± 0.05	0.395 ± 0.04
13	1	7	24	0.38 ± 0.06	3.34 ± 0.04	11.76 ± 0.04	0.391 ± 0.06
14	1	7	72	0.62 ± 0.02	3.39 ± 0.06	14.12 ± 0.01	0.388 ± 0.03
15	1	7	168	0.31 ± 0.03	3.31 ± 0.04	14.42 ± 0.02	0.384 ± 0.04
16	1	10	24	0.24 ± 0.12	3.23 ± 0.07	15.34 ± 0.03	0.381 ± 0.06
17	1	10	72	0.41 ± 0.14	3.28 ± 0.06	16.22 ± 0.05	0.378 ± 0.04
18	1	10	168	0.19 ± 0.09	3.18 ± 0.04	18.12 ± 0.03	0.371 ± 0.06

Table 3. Comparison of values predicted by RSM and ann for capillary absorption, thermal conductivity, compressive strength and flexural strength of bricks.

Mixture				Responses								
Runs	Factors			FS (MPa)			CS (MPa)			TC (W/m.K)		
	A-OFICP (%)	*B-NaHCO$_3$ T (°C)*	C-Duration (Hour)	EXP	ANN	RSM	EXP	ANN	RSM	EXP	ANN	RSM
1	0,5	5	24	0.56		0.57	3.42		3.44	0.581		0.592
2	0,5	5	72	0.73		0.7239	3.52		3.50	0.571		0.573
3	0,5	5	168	0.42		0.39	3.31		3.32	0.563		0.560
4	0,5	7	24	0.63		0.62	3.49		3.49	0.551		0.542
5	0,5	7	72	0.79		0.78	3.57		3.55	0.531		0.524
6	0,5	7	168	0.43		0.4681	3.36		3.38	0.511		0.510
7	0,5	10	24	0.42		0.44	3.34		3.36	0.461		0.453
8	0,5	10	72	0.64		0.61	3.43		3.42	0.421		0.435
9	1	10	168	0.23		0.21	3.19		3.19	0.401		0.382
10	1	5	24	0.33		0.31	3.29		3.27	0.399		0.397
11	1	5	72	0.44		0.49	3.32		3.35	0.396		0.388
12	1	5	168	0.25		0.23	3.23		3.23	0.395		0.395
13	1	7	24	0.38		0.38	3.34		3.33	0.391		0.397
14	1	7	72	0.62		0.58	3.39		3.42	0.388		0.388
15	1	7	168	0.31		0.33	3.31		3.29	0.384		0.395
16	1	10	24	0.241		0.23	3.23		3.22	0.381		0.384
17	1	10	72	0.41		0.44	3.28		3.30	0.378		0.376
18	1	10	168	0.19		0.21	3.18		3.19	0.371		0.382

(ANNs) mathematically and quantitatively mimic the neuronal activities of the human brain (Chai, Eisenbart, Nikzad, Fox, Blythe, Bwar, et al. 2023; Mebarkia et al. 2025b). These networks consist of several connected artificial neurons, each of which generates one output based on the data entered using a mathematical calculation. The back propagation multilayer ANN network uses observed FS, CS, and TC values as its output layer, while its input variables are OFICP%, NaHCO3%, and immersion duration. Feed-forward networks with backpropagation – a technique that converts and propagates data from the entrance layer to the exit layer – are commonly used in ANN training. Several steps are included in the backpropagation method' training phase until the lowest error rate is reached (Belaadi et al. 2023; Çolak et al. 2021). A multilayer perceptron (MLP) architecture is created by placing the neural network that represents the input parameters in the input layer, the hidden layer in the second layer, and the ANN outputs in the final layer (output layer). The hyperbolic kind is generally linked to the nonlinear fluctuation in transfer (f), as shown in (Eq. (4)).

$$f = \sum_{i=1}^{n} W_i X_i \tag{4}$$

where (n) represents the number of neurons, (Xi) the neurons' input parameters, and (Wi) the adjusted parameters.

The ANN architecture was created based on the toolbox in Matlab Neural Network. The input layer of the network is composed of three neurons, while the hidden layers for FS, CS, and TC are composed of six, ten, and eight neurons, respectively. The final layer, known as the exit layer, is made up of a single neuron that produces the output data. Three MLPs—3–6-1, 3–10-1, and 3–8-1—are utilized separately in this study to predict FS, CS, and TC responses, respectively. The applied MLP's structure is shown in Figure 5. The final layer, known as the exit layer, is made up of a single neuron that produces the output data. This process is carried out in the current study using the Levenberg-Marquadt (LM) algorithm. By applying activation functions to the total of the weighted inputs, a model ANN determines the value of an output. The network collected nonlinear relationships via the tanh activation methods of the buried layers (Chai et al. 2024). Genetic algorithmic approaches (GA) are algorithms designed to mimic the evolution of the human genetic system. By applying mutations, crossings, and choices to the population members, GAs search every region and make use of possible regions in order to address the issues of both linearity and non-linearity. The precision of an ANN model is assessed by calculating the difference in observed and predicted responses of the network. The coefficient of determination (R^2) is used for evaluating the ANN model. The two measurements are mean squared error (MSE) and root mean square error (RMSE) (Belaadi et al. 2023; Khelifi et al. 2024) (Eqs (5-7)).

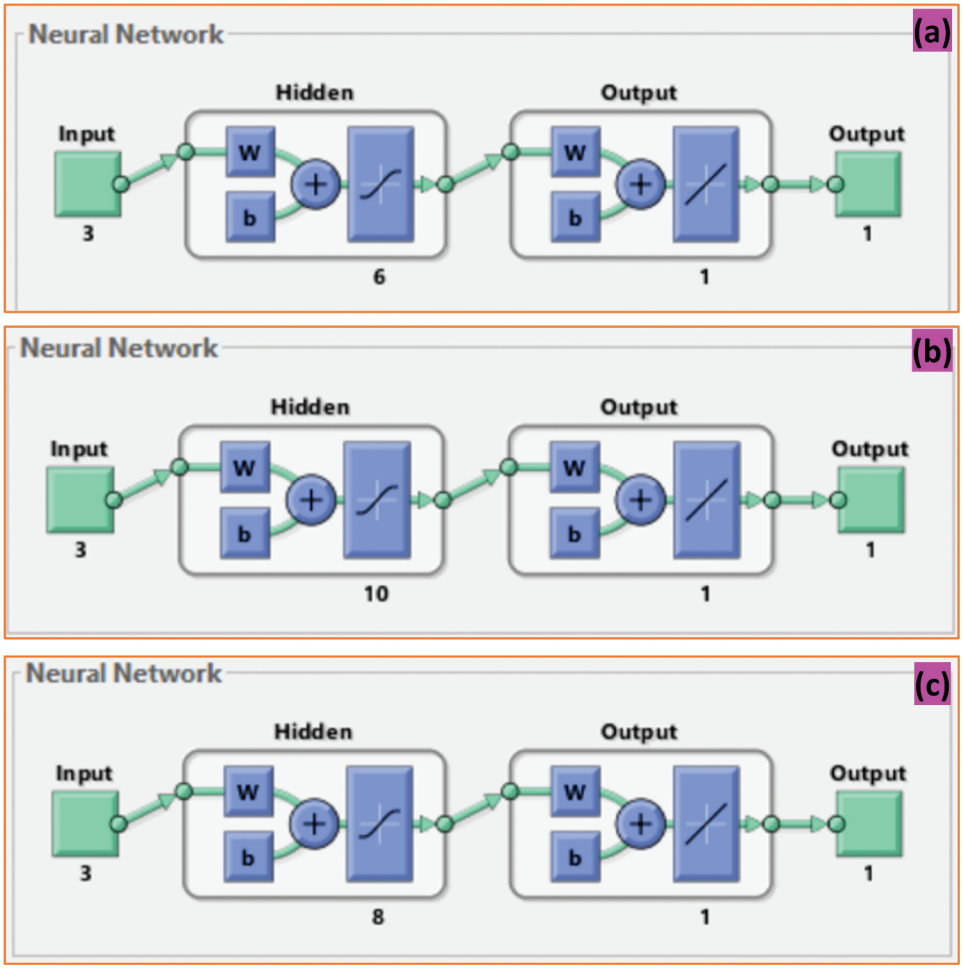

Figure 5. Artificial neural network (ANN) architecture for (a) flexural strength, (b) compressive strength and (c) thermal conductivity.

$$R^2 = \frac{\sum_1^n((Predictedi - Actual_i)}{\sum_{i=1}^n((Predictedi - Actual_i)^2} \quad (5)$$

$$RMSE = \sum_1^n \sqrt{\frac{(Predictedi - Actual_i)^2}{n}} \quad (6)$$

$$MSE = \sum_1^n \frac{(Predictedi - Actual_i)^2}{n} \quad (7)$$

Results and discussions

Mechanical characteristics of reinforced stabilized earth blocks

Figure 6a illustrates the impact of fiber dosage in the presence of 1% biochar by displaying the compressive strength (CS) of specimens containing 0.5% and 1% OFICP fibers. The 1% fiber formulation peaks at 3.395 MPa, while the formulation with 0.5% OFICP continuously performs better than the one with 1% OFICP, achieving a maximum compressive strength of 3.571 MPa. This implies that a moderate fiber content improves matrix cohesiveness and compaction, enabling the biochar to function as a micro-filler. On the other hand, compressive strength seems to decrease when the fiber concentration is increased to 1%, most likely as a result of fiber agglomeration or interference with particle packing. The alkaline treatment parameters – $NaHCO_3$ concentration and immersion time – also play a critical role. Comparatively, untreated fibers at the same doses produced lower compressive strengths (3.12 MPa for 0.5% OFICP and 3.01 MPa for 1% OFICP), suggesting that alkaline treatment greatly improves mechanical performance and fiber-matrix adhesion. The best results for 0.5% OFICP are obtained with 7% $NaHCO_3$ for 72 h, showing excellent surface activation of the fibers. A decrease in strength (e.g., 3.187 MPa at 168 h) is seen beyond this time or at greater concentrations (e.g., 10%), which may be caused by fiber deterioration or decreased interfacial bonding. A comparable pattern is observed for 1% OFICP, but with generally lower CS values, demonstrating that mechanical integrity can be jeopardized by high fiber concentration in conjunction with intensive or extended treatment. The findings indicate that the best compressive strength is obtained when 1% biochar and 0.5% OFICP fibers are mixed and treated in 7% NaHCO3 for 72 h. This is consistent with the findings of Mahgoub et al. (Salih, Osofero, and Imbabi 2020), who found that reinforced earth bricks performed better than unreinforced ones. In Taallah et al.'s research (Taallah and Guettala 2016), fibers treated with 0.05% alkali showed a 3.9% increase in compressive strength compared to untreated fiber

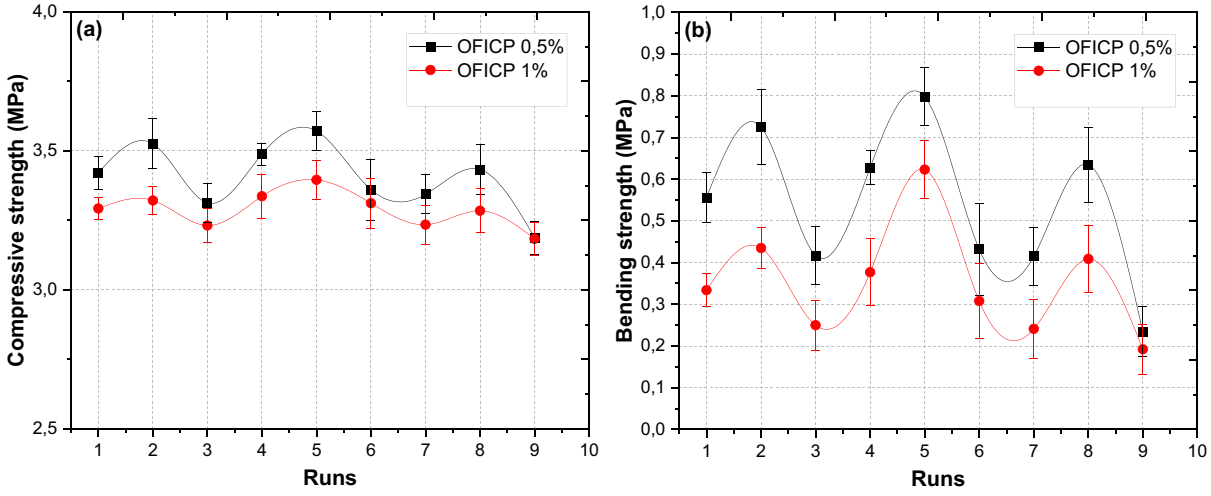

Figure 6. Impact of changing the fiber ratio on (a) compressive strength and (b) flexural strength of SEB stabilized with 1% biochar, 0.5 and 1% OFICP.

blocks. These findings support the improvement shown in the current investigation and confirm that alkaline treatment improves fiber-matrix adherence, leading to enhanced mechanical properties in bio-stabilized earth materials.

Figure 6b and Table 3 illustrate the effects of OFICP fiber dose, alkaline treatment conditions, and biochar addition on the bending strength (FS) of stabilized earth specimens. The baseline FS of the reference specimen without fibers or biochar is 0.37 MPa, whereas the addition of untreated OFICP fibers at 0.5% and 1% yields lower values of 0.34 MPa and 0.31 MPa, respectively. This decrease raises the possibility that untreated fibers could function as inert inclusions, impairing matrix cohesiveness without adding reinforcement. Alkali-treated fibers, on the other hand, greatly increase bending strength, particularly at 0.5% dosage. With 7% $NaHCO_3$ and 72 h of immersion, the highest FS value of 0.798 MPa is obtained, showing ideal surface activation and improved fiber-matrix adhesion. While extended immersion (168 h) or extreme alkalinity (10%) result in strength reduction (e.g., 0.234 MPa in Run 10), probably due to fiber breakdown or embrittlement, shorter immersion (24 h) and lower concentration (5%) offer moderate gains (e.g., 0.556 MPa). For 1% OFICP, the bending strength remains consistently lower than the 0.5% counterpart, with a maximum of 0.623 MPa. This suggests that excessive fiber content may hinder dispersion or create stress concentrations, limiting the reinforcement effect. Because of its tiny particle size, which increases packing density and decreases voids, the addition of 1% biochar to all formulations aids in matrix refining. When mixed with 0.5% treated OFICP fibers, its presence is especially advantageous since it enables the biochar to function as a micro-filler without sacrificing structural integrity. Nevertheless, the mechanical benefit is less noticeable when combined with 1% OFICP, most likely as a result of fiber overload and decreased compaction efficiency. These findings are in accordance with Kamwa et al.'s (2025) investigation, which found that stabilized earth bricks reinforced with 0.4 weight percent treated palm fibers demonstrated mechanical qualities appropriate for masonry applications. Their research showed that while excessive fiber addition may result in structural deterioration, low to moderate fiber contents (0.1–0.5 weight percent) increase strength.

Thermal and physical characteristics

Figure 7 shows the effect of varying fiber percentage on the capillary absorption and insulation characteristics of the SBS using alkali-treated fibers. The capillary water absorption coefficient (CA) data show that adding OFICP fibers along with 1% biochar significantly lowers the quantity of capillary-absorbed water (Figure 7a). For the control block (0% OFICP), the CA values varied from 8.12 g/cm^2 ·min$^{1/2}$ to 18.12 g/cm^2 ·min$^{1/2}$ for the formulation with 1% OFICP fibers and biochar. All tested formulations fall within the "weakly capillary" group (CA < 20) in accordance with the Standard NF XP P13-901 classification, which is

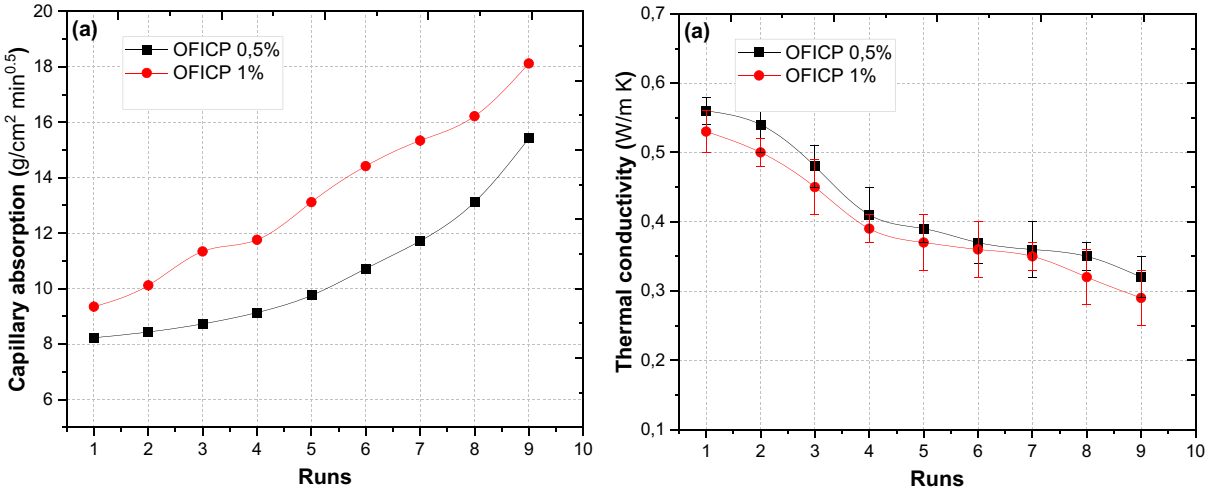

Figure 7. Impact of changing the fiber ratio on (a) water absorption coefficient and (b) thermal conductivity of SEB stabilized with 1% biochar, 0.5 and 1% OFICP.

advantageous for reducing moisture rise and improving long-term durability. This behavior is explained by the synergistic effect of natural fibers and biochar: the OFICP fibers, especially when treated, improve the internal structure without unduly increasing porosity, while the biochar functions as a micro-filler, decreasing pore connectivity and improving matrix densification. The CA value is somewhat higher when the fiber percentage is raised from 0.5% to 1%, but it is still below the critical threshold, indicating that the formulations maintain good resistance to capillary water infiltration. These results are in line with other research, such as that done by Khouja et al. (2021), who discovered that the addition of date palm waste to clay bricks increased their thermophysical performance.

The addition of OFICP fibers and biochar considerably decreased thermal conductivity, as seen in Figure 7b, with treated fibers at 1% dosage showing the lowest values. A conductivity of 0.64 W/m·K was found for control bricks, suggesting a comparatively high rate of heat transmission. The conductivity dropped to 0.48 W/m·K and 0.45 W/m·K, respectively, when untreated OFICP fibers were added at 0.5% and 1%, indicating the insulating effect of lignocellulosic materials. Nevertheless, conductivity values fell below 0.40 W/m·K in some tests when fibers were alkali-treated, especially with 7% $NaHCO_3$ for 72 h. Increased porosity, which obstructs thermal conduction channels, and improved fiber. This finding is in agreement with research by Khouja et al. (2021) that examined the thermophysical and mechanical characteristics of mud bricks made using date palm trash.

Thermal conductivity, flexural strength, and compressive strength modeling using response surface

The selection criteria defined for quadratic models are met because of their higher coefficients of correlation, adjusted R^2, and anticipated R^2. Equations 8–10 are generated from the second-degree polynomial equation that defined the responses obtained for FS, CS, and TC in accordance with the CCD, where the independent variables in the experimental design were coded as follows: A for the percentage of OFICP, B for the percentage of $NaHCO_3$, and C for the treatment duration.

$$FS = 0.7775 - 0.1767 \times A - 0.0690 \times B - 0.0889 \times C + 0.0388 \times AB + 0.0576 \times AC - 0.0031 \times BC - 0.1190 \times B - 0.2462 \times C \quad (8)$$

$$CS = 3.5301 - 0.1095 \times A - 0.0501 \times B - 0.0698 \times C + 0.0259 \times AB + 0.0506 \times AC - 0.0057 \times BC - 0.0927 \times B - 0.1109 \times C \quad (9)$$

$$TC = 0.5044 - 0.1172 \times A - 0.0732 \times B - 0.0195 \times C + 0.0632 \times AB + 0.0151 \times AC - 0.0055 \times BC - 0.0083 \times B + 0.0061 \times C \quad (10)$$

To ascertain the significance and nature of the correlations between the parameters, an analysis of variance (ANOVA) has been carried out for every response model (Table 4). The FS, CS, and TC models have ANOVA F-values of 50.66, 35.59, and 182.09, respectively, indicating perfect significance. Additionally, the *p*-values < 0.0001, which are significantly below 0.0500, confirm the relevance of the model terms. In the current model, terms A, B, C and AC have a considerable impact on compressive, bending strength, and thermal conductivity properties. The Adeq Precision values that permit the signal-to-noise rate of more than four for the FS, CS, and TC models in the current investigation are 24.1047, 20.2491, and 37.5232, respectively. These values make it possible to utilize models in the field of design and recommend a suitable signal.

Diagnostic graphs in connection to test datasets are also crucial for confirming the applicability and the quadratic models' quality of biochar-based bricks. The R^2 values for FS, CS, and TC, which are 97.69%, 98.56%, and 96.49%, respectively, demonstrate how well the regression model adapts to various testing data and provide a strong connection between expected and actual values. The corresponding adjusted R^2 values are 96.94%, 99.02%, and 97.83%. When the difference between the R^2 anticipated and fitted values is less than 0.2, each answer under investigation exhibits an acceptable degree of concordance. The brick compressive strength, flexural strength, and thermal conductivity models' real and expected value correlations, which are

Table 4. Variance analysis for capillary absorption, thermal conductivity, compressive strength and flexural strength of bricks.

Source	DF	SS	MS	F-value	Prob.	Remarks
a) Flexural strength.						
Model	8	0.5314	0.0664	50.66	<0.0001	Significant
A-OFICP	1	0.1149	0.1149	84.08	<0.0001	
B-$NaHCO_3$	1	0.0110	0.0110	8.06	0.0194	
C-Duration	1	0.0214	0.0214	15.63	0.0033	
AB	1	0.0022	0.0022	1.60	0.2372	
AC	1	0.0058	0.0058	4.21	0.0704	
BC	1	0.0009	0.0009	0.6290	0.4481	
B^2	1	0.0441	0.0441	32.28	0.0003	
C^2	1	0.1716	0.1716	125.60	<0.0001	
Residual	9	0.0123	0.0014			
Cor Total	17	0.5437				
SD = 0.0370					R^2 = 0.9783	
Mean = 0.4449					R^2 adjusted = 0.9590	
Coefficient of variation = 8.31					R^2 predicted = 0.9126	
					Adequate precision = 24.1047	
b) Compressive strength						
Model	8	0.2006	0.0251	35.59	<0.0001	significant
A-OFICP	1	0.0475	0.0475	81.56	<0.0001	
B-$NaHCO_3$	1	0.0056	0.0056	9.56	0.0129	
C-Duration	1	0.0131	0.0131	22.47	0.0011	
AB	1	0.0006	0.0006	0.9870	0.3464	
AC	1	0.0038	0.0038	6.54	0.0308	
BC	1	0.0001	0.0001	0.1053	0.7530	
B^2	1	0.0276	0.0276	47.31	<0.0001	
C^2	1	0.0342	0.0342	58.69	<0.0001	
Residual	9	0.0052	0.0006			
Cor Total	17	0.2059				
SD = 0.0241					R^2 = 0.9694	
Mean = 3.35.					R^2 adjusted = 0.9421	
Coefficient of variation = 0.7213					R^2 predicted = 0.8734	
					Adequate precision = 20.2491	
c) Thermal conductivity						
Model	8	0.1035	0.0129	182.09	<0.0001	significant
A-OFICP	1	0.0473	0.0473	341.62	<0.0001	
B-$NaHCO_3$	1	0.0175	0.0175	126.41	<0.0001	
C-Duration	1	0.0009	0.0009	6.55	0.0307	
AB	1	0.0092	0.0092	66.29	<0.0001	
AC	1	0.0005	0.0005	3.63	0.0892	
BC	1	2.273E-07	2.273E-07	0.0016	0.9686	
B^2	1	0.0001	0.0001	0.7673	0.4038	
C^2	1	0.0002	0.0002	1.61	0.2359	
Residual	9	0.0012	0.0001			
Cor Total	17	0.0005				
SD = 0.0118					R^2 = 0.9902	
Mean = 0.4486					R^2 adjusted = 0.9884	
Coefficient of variation = 4.62					R^2 predicted = 0.9747	
					Adequate precision = 37.5232	

displayed in Figure 8a–c, form an almost perfectly straight line, confirming the adequacy and sufficiency of quadratic models for these materials. The experimental results correspond closely to the forecasts. Figure 8d–f shows the residuals' trend in relation to anticipated outcomes. Based on the aforementioned data, the regression equations provided may accurately predict the variables FS, CS, and TC. Consequently, the response model developed is suitable and sufficient for predicting the FS, CS, and TC of bricks.

The contour and 3D response surfaces for FS, CS, and TC characteristics of the developed model are shown in Figure 9 as a function of two independent variables: treatment time and OFICP fiber percentage. The findings demonstrate that when the percentage of OFICP rises, flexural strength (FS) and compressive strength (CS) decline. Furthermore, as the immersion time above a crucial threshold of around 96 h, these mechanical qualities tend to deteriorate. Similar trends are seen in thermal conductivity (TC), which falls with increasing OFICP content and treatment duration. The detrimental effects of excessive OFICP are shown in these behaviors. The 3D response surfaces indicate the optimal areas where the combined effects of treatment duration and OFICP fiber fraction improve mechanical performance while minimizing conductivity. These findings are in line with prior research

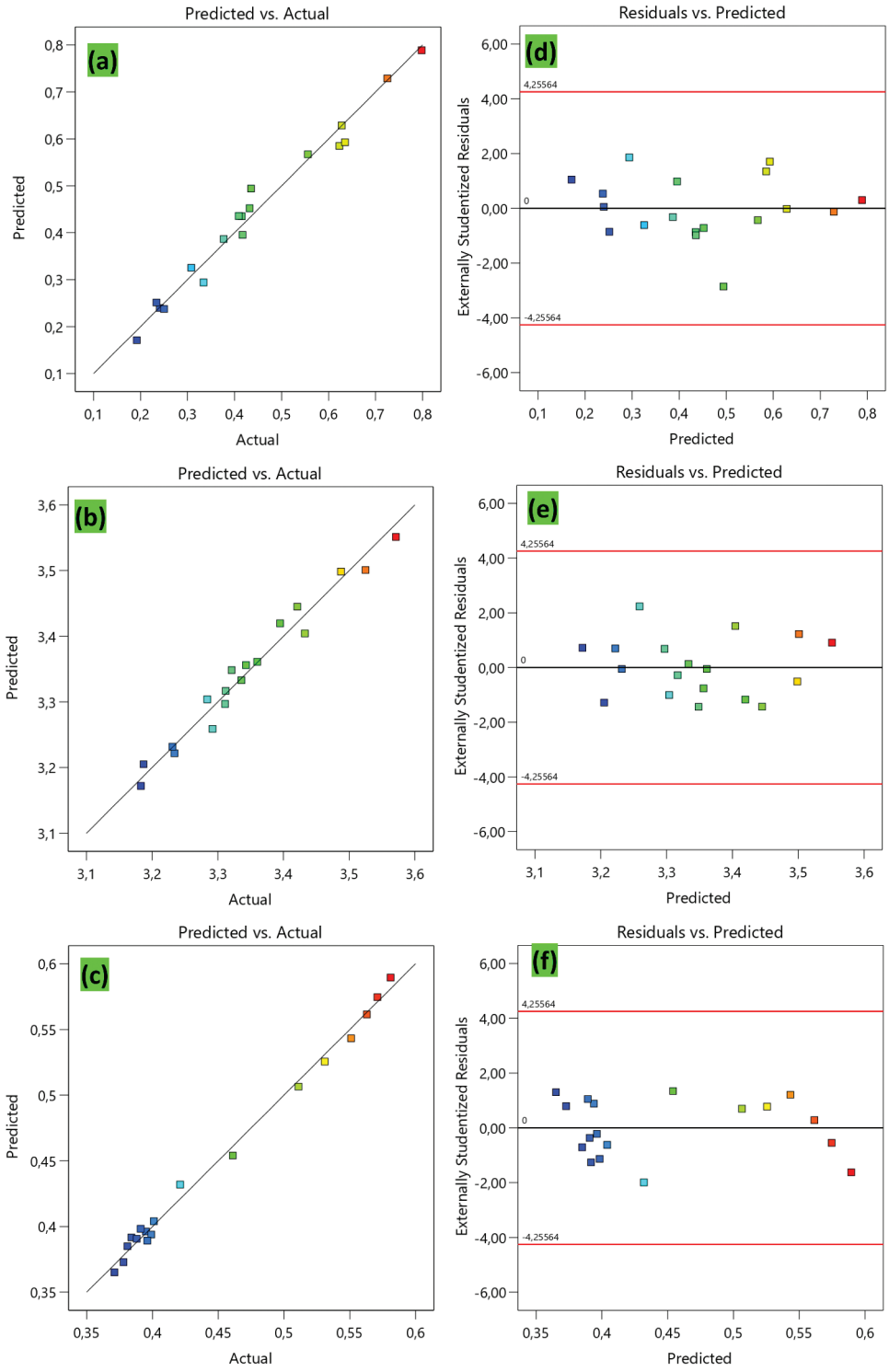

Figure 8. Diagnosis of the bricks compressive, flexural strength and thermal conductivity models : (a-c) predictions vs. actuals, and (d-f) residuals vs. predictions.

demonstrating that excessive additions of natural fibers can degrade the mechanical and thermal performance of composites, mostly because of adhesion flaws and fiber agglomerations (Anand, Gopalan, and Pitchumani 2025). This demonstrates the importance of it is to strike the ideal balance between processing time and OFICP fiber content in order to maximize material performance and minimize heat conductivity. Consequently, RSM results confirm that the experimental and projected outcomes are in good accord.

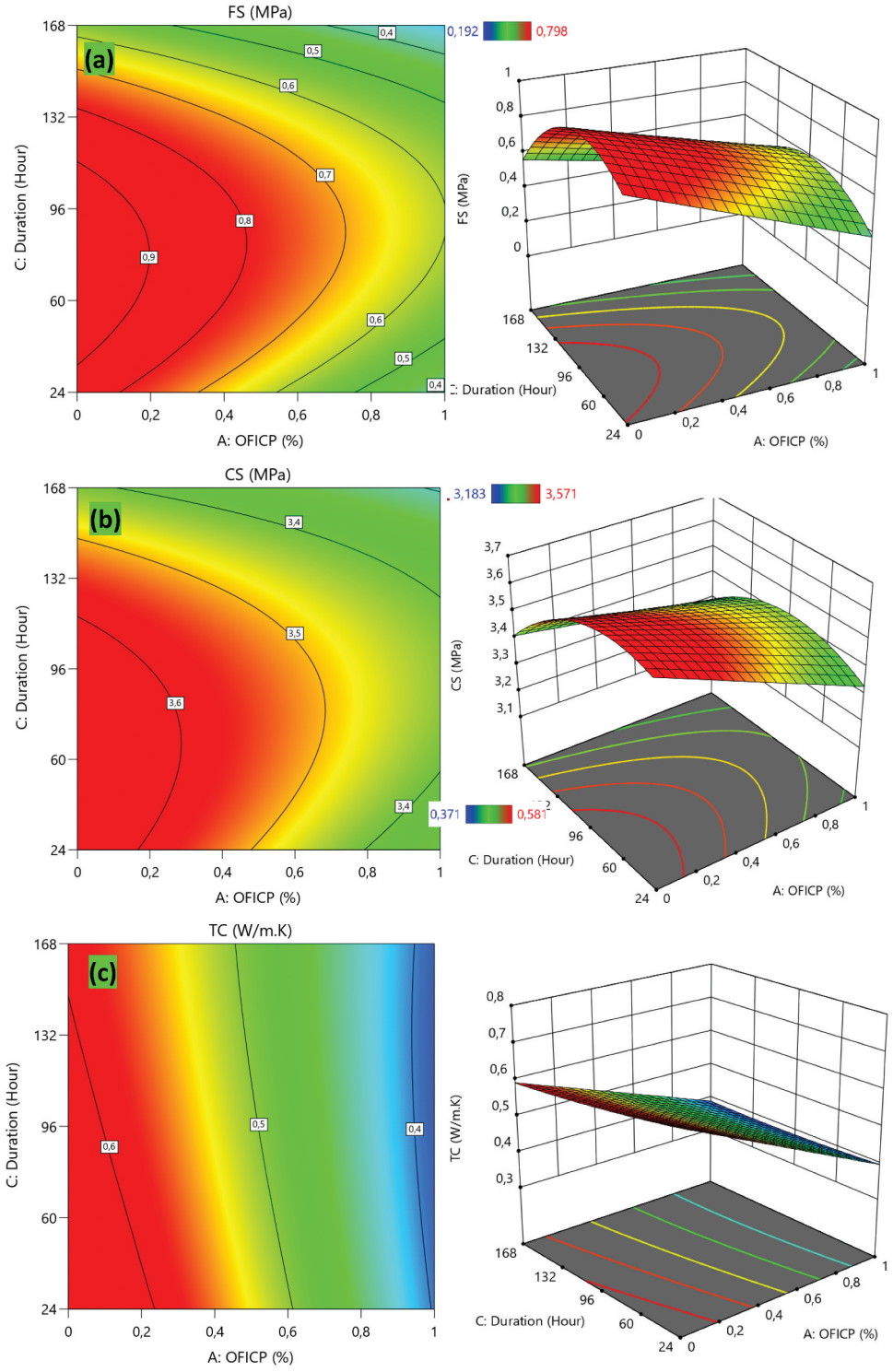

Figure 9. Contour plots and 3D of response surfaces: (a) flexural strength, (b) compressive strength and (c) thermal conductivity.

Artificial intelligence using neural networks

The data set was ran three times for learning, testing and validation. In order to assess the network's performance, the experimental plan comprised 18 runs: 12 for network training (70%), 3 for testing (15%), and 3 for validating (15%). Neural network training was done using the backpropagation technique with a falling gradient, learning ratio $\eta = 0.1$, and iteration = 100. Due to their speed and minimal memory

consumption, the (TRAINLM) LM algorithms were chosen for learning. The tangent hyperbolic sigmoid transfer function (TANSIG) served as the means of activating function.

The datasets used for testing and learning during the development process of the model is listed in Table 5. To evaluate the efficacy of ANN models, the findings of the study of actual and projected data are shown in Figure 10 and Table 3. The expected and actual outcomes were shown to fit each other satisfactorily. The equivalent correlation coefficients for the learning, validation, test, and entire data sets for FS, CS, and TC predicted vs. actual data are 0.9946, 0.9997, 0.9722, and 0.9908; 0.9961, 0.9999, 0.9736, and 0.9923; and 0.9998, 0.9946, 0.9999, and 0.9940. Strong correlations among the actual and predicted findings are indicated by R2 values. Based on the results of experiments, the created ANN models (Table 6) had the capacity to anticipate outcomes with high accuracy. The error rate calculation represents an essential performance evaluation aspect, based on the discrepancy between predictions and actual results. The MSE value rose at the start of the artificial neural network learning process and decreased at its conclusion (Figure 11a–c). The MSE values for FS, CS, and TC dropped during the ninth, fourth, and fifth epochs, respectively, when the optimal adjustment line was matched to the learning, confirmation, and testing phases. The ANN training procedure was then completed. Figure 11d–f depict the zero-error zone, which has the fewest errors. There was a performance. Several faults were introduced to demonstrate performance throughout the ANN network development phase. This finding is consistent with earlier study utilizing artificial neural networks (Armaghani and Asteris 2021; Eskandari-Naddaf and Kazemi 2017; Kooshkaki and Eskandari-Naddaf 2019). The results confirm the ability of the models to accurately predict mechanical and thermal performance based on the selected inputs. This research shows practical implementation using RSM with ANN models in brick manufacturing, demonstrating their potential to achieve specific performance targets.

The accuracy and usefulness of the model

The validity of the models was further evaluated by contrasting the outcomes with those derived from the RSM and ANN techniques. Based on graphs made from the values given in each test result, the model generated predictions which were reasonably close to the actual data. Consequently, the ANN model can perform better than the RSM model in terms of dataset extrapolation. The ANN method makes it possible to accurately forecast and validate experimental data in order to evaluate the mechanical and thermal properties of the bricks. The appropriateness of the ANN and RSM models was assessed by analyzing the R^2, MSE, and RMSE. When a model's R^2 coefficients approach one, it is often seen to be more effective for projecting responses (X. Li et al. 2025). Table 7 shows the degree of statistical significance as well as the encouraging outcomes from the ANN and RSM algorithms when applied to the observed data. The R^2 values of the ANN model exceed those of the RSM model. RSM produces R^2 (0.9783, 0.9694, and 0.9902) and MSE (0.2456, 0.3215, and 0.4823) for FS, CS, and TC, respectively, whereas ANN produces R^2 (0.9908, 0.9922, and 0.9940) and MSE (0.0985, 0.0176, and 0.1243). The RMSE errors for each model were also investigated (Aydoğmuş, Arslanoğlu, and Dağ 2021).

Brick optimization using the RSM and ANN method

To determine which of the FS, CS, and TC reactions was most suited, the RSM technique was utilized to calculate optimal values for both parameters (OFICP %, NaHCO3% and duration). The RSM optimization

Table 5. ANN data processing details.

Model	Network architecture		Percentage	Samples	*MSE*	*R* value
Flexural strength	3–6–1	Training	70	12	3.53426E-04	0.9946
		Validation	15	3	1.84123E-05	0.9997
		Testing	15	3	2.15462E-06	0.9722
Compressive strength	3–10–1	Training	70	12	1.57864E-05	0.9961
		Validation	15	3	2.36547E-05	0.9999
		Testing	15	3	2.23654E-03	0.9736
Thermal conductivity	3–8–1	Training	70	12	3.65732E-06	0.9998
		Validation	15	3	6.53452E-04	0.9946
		Testing	15	3	1.96780E-04	0.9999

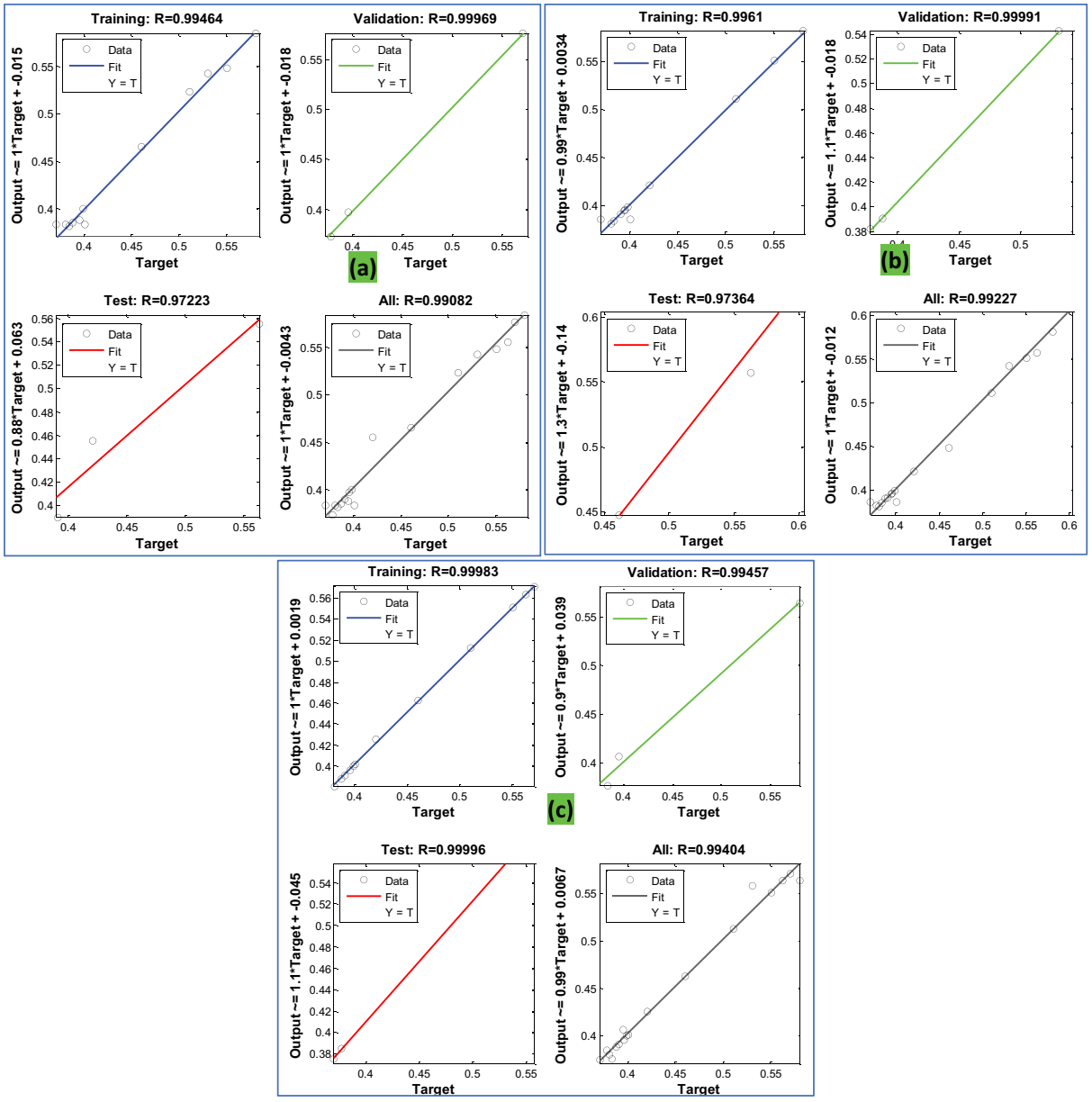

Figure 10. ANN models' real vs predicted values for training, validation, testing and the entire data set: (a) for bending strength, (b) compressive strength and (c) thermal conductivity respectively.

technique leverages the desirability function (DF) feature of the Design Expert software. A double goal optimization technique generates a design that satisfies lower and upper constraints simultaneously (Chai, Eisenbart, Nikzad, Fox, Blythe, Blanchard, et al. 2023). Tables 8 and 9 and Figure 12 show the optimal OFICP%, NaHCO3%, and duration levels for the FS, CS, and TC outcomes. The exceptional values for FS, CS, and TC were 0.68 MPa, 3.47 MPa, and 0.44 W/K.m, respectively. Results showed that 0.78%, 7.62%, and 89.33 h were the optimal values for OFICP content, $NaHCO_3$ concentration, and duration, respectively.

GAs are based on biological choice and genetic mechanisms. A group of viable starting points (chromosomes) that may be evaluated for capability (ability) make up the first selection point. Selection, crossover, and mutation are three main progress approaches which can be utilized to create a set of potential alternatives (Z. Wang and Sobey 2020). This research used a GA method to increase thermal and mechanical characteristics while also determining the optimal OFICP%, $NaHCO_3$% and duration. The GA's mutation, crossover, and total population adjusted statistics were 0.01, 100, and 0.70. The choice, mutation and crossover processes were chosen using roulette, uniform and heuristic, approaches. Table 9 displays the

Table 6. The mathematical predictions produced by the ANN for the bricks' compressive, bending, and thermal conductivity strengths.

ANN responses	Mathematical models
Flexural strength	$0.089 \times H1 + 0.311 \times H2 + 0.505 \times H3 - 0.636 \times H4 - 0.760 \times H5 + 0.282 \times H6 - 0.390$
	$H1 = \tanh(.5 \times (-4.763 \times OFICP + 0.847 \times NaHCO3 - 0.013 \times Duration - 2.512))$
	$H2 = \tanh(.5 \times (1.381 \times OFICP - 0.802 \times NaHCO3 - 0.001 \times Duration + 6.535))$
	$H3 = \tanh(.5 \times (-5.745 \times OFICP - 0.131 \times NaHCO3 - 0.009 \times Duration + 5.486))$
	$H4 = \tanh(.5 \times (-1.533 \times OFICP + 0.050 \times NaHCO3 - 0.029 \times Duration + 1.356))$
	$H5 = \tanh(.5 \times (-1.613 \times OFICP - 0.070 \times NaHCO3 + 0.011 \times Duration - 0.325))$
	$H6 = \tanh(.5 \times (0.184 \times OFICP + 0.462 \times NaHCO3 + 0.006 \times Duration - 2.689))$
Compressive strength	$-0.253 \times H1 + 0.080 \times H2 + 0.201 \times H3 + 0.146 \times H4 + 0.005 \times H5 - 0.058 \times H6 + 0.228 \times H7 - 0.779 \times H8 + -0.319 \times H9 + 0.447 \times H10 + 2.495$
	$H1 = \tanh(.5 \times (1.349 \times OFICP - 0.410 \times NaHCO3 - 0.006 \times Duration + 2.112))$
	$H2 = \tanh(.5 \times (8.302 \times OFICP + 0.619 \times NaHCO3 - 0.004 \times Duration - 9.852))$
	$H3 = \tanh(.5 \times (-4.532 \times OFICP - 0.434 \times NaHCO3 - 0.022 \times Duration + 9.842))$
	$H4 = \tanh(.5 \times (4.992 \times OFICP + 0.441 \times NaHCO3 + 0.014 \times Duration - 9.244))$
	$H5 = \tanh(.5 \times (4.265 \times OFICP + 0.730 \times NaHCO3 + 0.020 \times Duration - 10.38))$
	$H6 = \tanh(.5 \times (1.679 \times OFICP - 0.678 \times NaHCO3 + 0.006 \times Duration + 2.899))$
	$H7 = \tanh(.5 \times (-0.304 \times OFICP - 1.070 \times NaHCO3 + 0.010 \times Duration + 8.949))$
	$H8 = \tanh(.5 \times (1.699 \times OFICP - 0.001 \times NaHCO3 + 0.008 \times Duration - 4.183))$
	$H9 = \tanh(.5 \times (-4.357 \times OFICP + 0.050 \times NaHCO3 + 0.033 \times Duration - 2.947))$
	$H10 = \tanh(.5 \times (-1.540 \times OFICP - 0.089 \times NaHCO3 + 0.012 \times Duration - 0.088))$
Thermal conductivity	$-0.235 \times H1 + -0.279 \times H2 + 0.461 \times H3 + 0.031 \times H4 + 0.125 \times H5 + 0.397 \times H6 + -0.167 \times H7 + -0.304 \times H8 + 0.577$
	$H1 = \tanh(.5 \times (0.166 \times NaHCO3 + 0.028 \times Duration - 0.047 \times Flexural\_strength\_MPa - 3.173))$
	$H2 = \tanh(.5 \times (0.290 \times NaHCO3 - 0.011 \times Duration - 0.862 \times Flexural\_strength\_MPa - 0.808))$
	$H3 = \tanh(.5 \times (0.180 \times NaHCO3 + 0.023 \times Duration - 0.164 \times Flexural\_strength\_MPa - 4.483))$
	$H4 = \tanh(.5 \times (-1.028 \times NaHCO3 + 0.001 \times Duration + 1.779 \times Flexural\_strength\_MPa + 7.804))$
	$H5 = \tanh(.5 \times (0.017 \times NaHCO3 + 0.012 \times Duration + 1.218 \times Flexural\_strength\_MPa + 0.934))$
	$H6 = \tanh(.5 \times (-0.192 \times NaHCO3 + 0.003 \times Duration - 0.003 \times Flexural\_strength\_MPa + 2.082))$
	$H7 = \tanh(.5 \times (-0.927 \times NaHCO3 + 0.019 \times Duration + 0.533 \times Flexural\_strength\_MPa + 7.011))$
	$H8 = \tanh(.5 \times (-0.085 \times NaHCO3 + 0.022 \times Duration + 0.142 \times Flexural\_strength\_MPa - 1.035))$

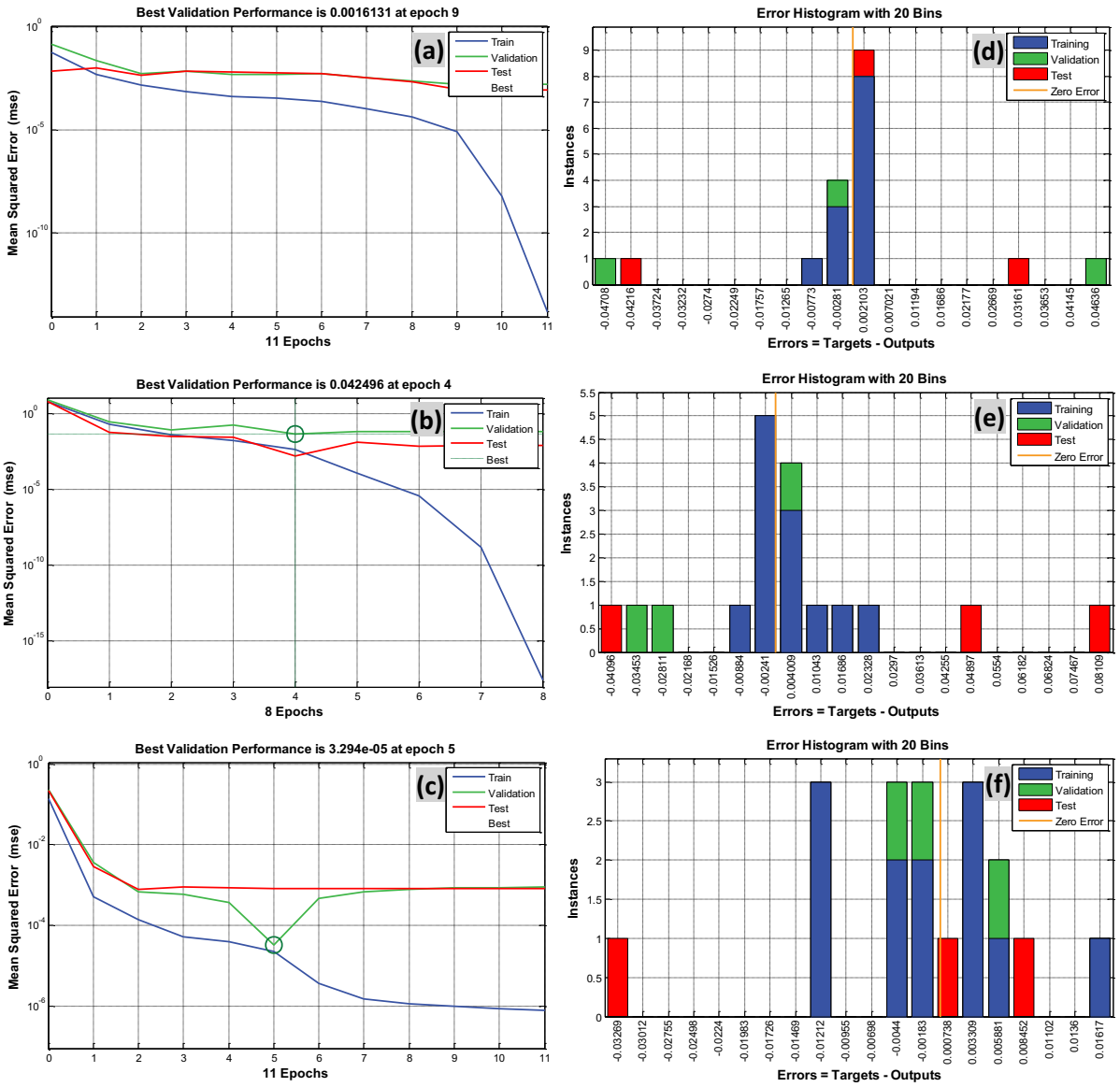

Figure 11. Mean square error and variation histogram fluctuation with respect to time for the following: (a – d) bending strength; (b – e) compressive strength; and (c – f) thermal conductivity.

Table 7. R^2, mean squared error (MSE), and root mean square error (RMSE) of mechanical and thermal properties of bricks calculated using RSM and ANN.

	R^2		MSE		RMSE	
Responses	RSM	ANN	RSM	ANN	RSM	ANN
FS	0.9783	0.9908	0.2456	0.0985	0.1143	0.0947
CS	0.9694	0.9922	0.3215	0.0176	0.0587	0.0324
TC	0.9902	0.9940	0.4823	0.1243	0.3756	0.0198

best variable values (OFICP content = 0.5%, $NaHCO_3$ concentration = 7.48%, and duration = 80.11 h), as well as the ideal values for TC, FS, and CS, which are 0.55 W/K.m, 0.81 MPa, and 3.56 MPa. The results showed that the ANN/GA technique provided the highest CS (3.59 MPa) and FS (0.85 MPa) when compared to the CS (3.55 MPa) and FS (0.79 MPa) obtained by RSM/DF. The ideal OFICP content, NaHCO3%, and duration levels were comparable across both techniques. ANN/GA's somewhat improved performance can be attributed to its ability to identify non-linear and complex relationships within outputs

Table 8. Optimization variables' goals and variations.

Title	Objective	Lower level	Upper level
OFICP content biochar	is in range	0.5	1
$NaHCO_3$ percentage	is in range	5	10
Duration	is in range	24	168
FS	maximize	0.19	0.78
CS	maximize	3.18	3.57
TC	minimize	0.37	0.58

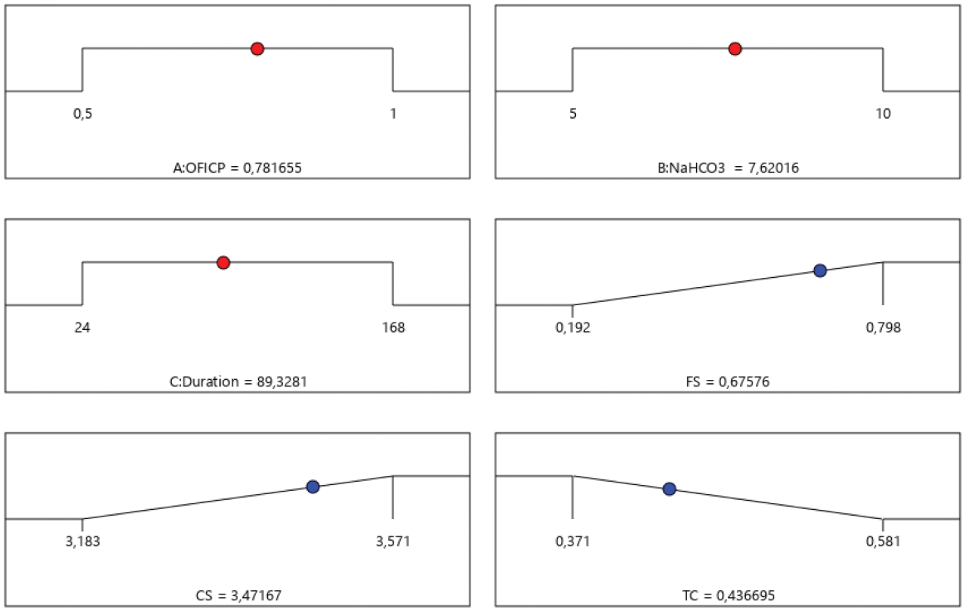

Figure 12. The best responses of thermal conductivity, flexural stress, and compressive stress utilizing anticipated ramping.

Table 9. Optimization settings and experimental findings.

		Input variables			Responses	
Name	OFICP content (%)	$NaHCO_3$ percentage (%)	Duration (Hour)	FS (MPa)	CS (MPa)	TC (W/K.m)
Objective	In range	In range		Maximum	Maximum	Minimum
Optimization RSM/DF	0.78	7.62	89.33	0.68	3.47	0.44
Optimization ANN/GA	0.5	7.48	80.11	0.85	3.59	0.55
Experimental tests	0.5	7.5	80	0.84	3.57	0.56

and inputs. RSM/DF is recommended for faster and easier optimization procedures due to its fundamental polynomial modeling method, but ANN/GA is advised for sophisticated systems requiring better precision due to its power to represent nonlinear patterns of data (Y. Wang et al. 2022).

Conclusion

This study emphasizes the potential of bio-sourced materials as a long-lasting building material, particularly raw earth bricks reinforced with *Opuntia ficus-indica* cactus plant and biochar produced by the same waste plant. A rigorous full factorial design was employed, combined with Response Surface Methodology (RSM) and Artificial Neural Networks (ANN), to systematically evaluate the influence of OFICP%, $NaHCO_3$%, and immersion period on brick performance. Optimizing fiber content and alkaline treatment conditions improves matrix-fiber cohesion and compactness of SEBs bricks.

The formulation with 1% biochar and 0.5% treated fibers (7% $NaHCO_3$, 72 h) had the highest compressive strength (CS: 3.571 MPa) and bending strength (FS: 0.798 MPa). A high fiber concentration

(1%) or an overly aggressive alkaline treatment can affect the mechanical integrity of the SEBs bricks, whereas untreated fibers have inferior mechanical properties, demonstrating the efficiency of alkaline treatment in increasing matrix-fiber adhesion.

The use of biochar and *Opuntia ficus-indica* cactus waste increase the capillary absorption of SEBs bricks. The 0.5% and 1% formulations exhibit higher absorption than the fiber-free control (CA = 8.12 $g/cm^2 \cdot m^{0.5}$), with the 1% concentration continuously surpassing the 0.5%. The capillary absorption coefficient (CA) for all formulations is below the essential threshold of 20 $g/cm^2 \cdot min^{1\,2}$, indicating their appropriateness for construction applications.

As the proportion of OFICP waste increases, thermal conductivity of SEBs decreases significantly – from 0.46 to 0.22 W/m·K for the 0.5% formulations, and from 0.43 to 0.21 W/m·K for the 1% formulations – highlighting the insulating effect of its microporous structure. Predictive quadratic models achieved R^2 values up to 96%, confirming strong accuracy, while ANN outperformed RSM by yielding lower RMSE and MSE values. Multi-criteria optimization identified optimal manufacturing conditions at 0.44% OFICP, 7.48% $NaHCO_3$, and 80.11 h of immersion, ensuring a balance between thermal insulation and mechanical strength.

The combination of biochar and *Opuntia ficus-indica* fibers has been particularly effective in increasing the mechanical and thermal performance of raw SEBs bricks while also utilizing local plant waste. This strategy improves both the materials' energy efficiency and their environmental sustainability.

Beyond the findings, a number of research directions should be investigated. First, long-term durability tests (freeze/thaw cycles, accelerated aging, chemical agent resistance) will verify the formulations' resilience in practical settings. Second, using additional local biomass or agricultural waste could increase circularity and expand the range of bio-based materials. To compare these bricks with traditional materials in terms of cost, carbon footprint, and energy performance, a thorough economic and technical-environmental analysis, including a life cycle assessment (LCA), would be required.

Abbreviations

OFICP	*Opuntia ficus-indica* cactus plant.
SEB	Stabilized earth bricks
CEB	Compressed earth blocks
ANN	Artificial Neural Network
MLP	Multi-Layer Perceptron
RSM	Response Surface Methodology
ANOVA	Analysis of Variance
CCD	Central Composite Design
DF	Desirability function
MS	Mean squares
p-value	Probability value
F-value	Fisher value
SD	Standard deviation
SS	Sum of squares
RMSE	Root Mean Squared Error
MSE	Mean Squared Error
R^2	Coefficient of determination

Acknowledgments

The authors, therefore, acknowledge with thanks DSR for technical and financial support.

Author contributions

CRediT: **Hocine Boudjehm:** Conceptualization, Formal analysis, Investigation, Methodology, Validation, Writing – original draft; **Messaouda Boumaaza:** Formal analysis, Investigation, Methodology, Resources, Validation, Writing – original draft; **Ahmed Belaadi:** Data curation, Methodology, Supervision, Validation, Visualization, Writing – review & editing; **Wail Harasani:** Validation, Visualization, Writing – review & editing; **Mostefa Bourchak:** Validation,

Visualization, Writing – review & editing; **Ibrahim M. H. Alshaikh:** Validation, Visualization, Writing – review & editing; **Djamel Ghernaout:** Validation, Visualization, Writing – review & editing.

Disclosure statement

No potential conflict of interest was reported by the author(s).

Funding

his Project was funded by the Deanship of Scientific Research (DSR) at King Abdulaziz University, Jeddah, under grant no. [IPP:1418-135-2025]. The authors, therefore, acknowledge with thanks DSR for technical and financial support.

ORCID

Messaouda Boumaaza http://orcid.org/0000-0003-3349-2307

References

Abdeldjebar, R., A. Hamouine, F. Fouchal, and B. Labbaci. 2018. "Effects of Treated Date Palm Fiber on Durability of Stabilized Earth Blocks (SEB)." *International Journal of Civil Engineering and Technology (IJCIET)* 9 (5): 293–305. http://www.iaeme.com/IJCIET.

Alioui, A., M.-A. Babay, M. Benfars, Y. Azalam, S. Idrissi Kaitouni, E. M. Bendada, and M. Mabrouki. 2026. "Prediction and Optimization of the Thermomechanical Performance of Carbon-Free Adobe Bricks Reinforced With Straw and Sawdust Using Machine Learning." *Scientific African* 31:e03167. https://doi.org/10.1016/j.sciaf.2025.e03167.

Anand, S., V. Gopalan, and S. V. Pitchumani. 2025. "Optimization of Thermal Conductivity in Coir Fibre-Reinforced PVC Composites Using Advanced Computational Techniques." *Scientific Reports* 15 (1): 16675. https://doi.org/10.1038/s41598-025-01471-8.

Aparicio, J. G., E. G. D. L. Monter, N. O. Lara, R. E. Garcia, and M. N. Rojas-Valencia. 2019. "Study of the Properties of the Echerhirhu-Block Made with Opuntia Ficus Mucilage for Use in the Construction Industry." *Case Studies in Construction Materials* 10:e00216. https://doi.org/10.1016/j.cscm.2019.e00216.

Armaghani, D. J., and P. G. Asteris. 2021. "A Comparative Study of ANN and ANFIS Models for the Prediction of Cement-Based Mortar Materials Compressive Strength." *Neural Computing & Applications* 33 (9): 4501–4532. https://doi.org/10.1007/s00521-020-05244-4.

Ashour, T., A. Korjenic, S. Korjenic, and W. Wu. 2015. "Thermal Conductivity of Unfired Earth Bricks Reinforced by Agricultural Wastes with Cement and Gypsum." *Energy & Buildings* 104:139–146. https://doi.org/10.1016/j.enbuild.2015.07.016.

Aydoğmuş, E., H. Arslanoğlu, and M. Dağ. 2021. "Production of Waste Polyethylene Terephthalate Reinforced Biocomposite with RSM Design and Evaluation of Thermophysical Properties by ANN." *Journal of Building Engineering* 44:103337. https://doi.org/10.1016/j.jobe.2021.103337.

Baibordy, A., M. Yekrangnia, and S. G. Jahromi. 2025. "A Comprehensive Study on the Mechanical Properties of Natural Fiber Reinforced Stabilized Rammed Earth Using Experimental and Data-Driven Fuzzy Logic-Based Analysis." *Cleaner Materials* 15:100300. https://doi.org/10.1016/j.clema.2025.100300.

Bamogo, H., M. Ouedraogo, I. Sanou, K. A. J. Ouedraogo, K. Dao, J.-E. Aubert, and Y. Millogo. 2020. "Improvement of Water Resistance and Thermal Comfort of Earth Renders by Cow Dung: An Ancestral Practice of Burkina Faso." *Journal of Cultural Heritage* 46:42–51. https://doi.org/10.1016/j.culher.2020.04.009.

Belaadi, A., M. Boumaaza, H. Alshahrani, and M. Bourchak. 2023. "Optimization of Palm Rachis Biochar Waste Content and Temperature Effects on Predicting Bio-Mortar: ANN and RSM Modelling." *Journal of Natural Fibers* 20 (1): 2151547. https://doi.org/10.1080/15440478.2022.2151547.

Boumaaza, M., A. Belaadi, H. Alshahrani, M. K. A. Khan, and M. Jawaid. 2024. "Environmentally Mortar Development Using Washingtonia/Biochar Waste Hybrid: Mechanical and Thermal Properties." *Biomass Conversion and Biorefinery* 14 (23): 30125–30148. https://doi.org/10.1007/s13399-023-04743-3.

Boumaaza, M., A. Belaadi, M. Bourchak, M. Jawaid, and S. Hamid. 2022. "Comparative Study of Flexural Properties Prediction of Washingtonia Filifera Rachis Biochar Bio-Mortar by ANN and RSM Models." *Construction and Building Materials* 318:125985. https://doi.org/10.1016/J.CONBUILDMAT.2021.125985.

CDE. 2000. *ENTPE, Compressed Earth Blocks: Testing Procedures Guide-Technology Series N 16*. Brussels-Belgium: CDE (ARSO).

Chai, B. X., B. Eisenbart, M. Nikzad, B. Fox, A. Blythe, P. Blanchard, and J. Dahl. 2023. "A Novel Heuristic Optimisation Framework for Radial Injection Configuration for the Resin Transfer Moulding Process."

Composites, Part A, Applied Science and Manufacturing 165:107352. https://doi.org/10.1016/J.COMPOSITESA.2022.107352.

Chai, B. X., B. Eisenbart, M. Nikzad, B. Fox, A. Blythe, K. H. Bwar, J. Wang, Y. Du, and S. Shevtsov. 2023. "Application of KNN and ANN Metamodeling for RTM Filling Process Prediction." *Materials* 16 (18): 6115. https://doi.org/10.3390/ma16186115.

Chai, B. X., J. Wang, T. K. M. Dang, M. Nikzad, B. Eisenbart, and B. Fox. 2024. "Comprehensive Composite Mould Filling Pattern Dataset for Process Modelling and Prediction." *Journal of Composites Science* 8 (4): 153. https://doi.org/10.3390/jcs8040153.

Chihab, Y., N. Laaroussi, and M. Garoum. 2023. "Thermal Performance and Energy Efficiency of the Composite Clay and Hemp Fibers." *Journal of Building Engineering* 73:106810. https://doi.org/10.1016/j.jobe.2023.106810.

Çolak, A. B., K. Akçaözoğlu, S. Akçaözoğlu, and G. Beller. 2021. "Artificial Intelligence Approach in Predicting the Effect of Elevated Temperature on the Mechanical Properties of PET Aggregate Mortars: An Experimental Study." *Arabian Journal for Science & Engineering* 46 (5): 4867–4881. https://doi.org/10.1007/s13369-020-05280-1.

Danso, H., D. B. Martinson, M. Ali, and J. B. Williams. 2015a. "Effect of Fibre Aspect Ratio on Mechanical Properties of Soil Building Blocks." *Construction and Building Materials* 83:314–319. https://doi.org/10.1016/j.conbuildmat.2015.03.039.

Danso, H., D. B. Martinson, M. Ali, and J. B. Williams. 2015b. "Physical, Mechanical and Durability Properties of Soil Building Blocks Reinforced with Natural Fibres." *Construction and Building Materials* 101:797–809. https://doi.org/10.1016/j.conbuildmat.2015.10.069.

Dao, K., M. Ouedraogo, Y. Millogo, J.-E. Aubert, and M. Gomina. 2018. "Thermal, Hydric and Mechanical Behaviours of Adobes Stabilized with Cement." *Construction and Building Materials* 158:84–96. https://doi.org/10.1016/j.conbuildmat.2017.10.001.

Dime, T., S. O. Sore, P. Nshimiyimana, A. Messan, and L. Courard. 2022. "Comparative Study of the Reactivity of Clay Earth Materials for the Production of Compressed Earth Blocks in Ambient Conditions: Effect on Their Physico-Mechanical Performances." *Journal of Minerals and Materials Characterization and Engineering* 10 (1): 43. https://doi.org/10.4236/jmmce.2022.101004.

Eskandari-Naddaf, H., and R. Kazemi. 2017. "ANN Prediction of Cement Mortar Compressive Strength, Influence of Cement Strength Class." *Construction and Building Materials* 138:1–11. https://doi.org/10.1016/j.conbuildmat.2017.01.132.

Ganasen, N., L. Krishnaraj, K. C. Onyelowe, and L. U. Stephen. 2024. "Machine Learning Optimization of Bio-Sandcrete Brick Modelling Using Response Surface Methodology." *Scientific Reports* 14 (1): 3438. https://doi.org/10.1038/s41598-024-54029-5.

Gavali, H. R., A. Bras, P. Faria, and R. V. Ralegaonkar. 2019. "Development of Sustainable Alkali-Activated Bricks Using Industrial Wastes." *Construction and Building Materials* 215:180–191. https://doi.org/10.1016/j.conbuildmat.2019.04.152.

Ghadir, P., and N. Ranjbar. 2018. "Clayey Soil Stabilization Using Geopolymer and Portland Cement." *Construction and Building Materials* 188:361–371. https://doi.org/10.1016/j.conbuildmat.2018.07.207.

Gueffaf, N., B. Rabehi, M. Boumaaza, K. Boumchedda, A. Belaadi, M. S. Abdullah, M. Klimkina, I. A. Al-Lohedan, A. Al-Khawlani, and Y. H. Chetbani. 2025. "Performance of Earth Blocks Based on Recycled Dam Sediment and Reinforced with Alfa Fibers: Experimental Study." *Journal of Natural Fibers* 22 (1): 2512002. https://doi.org/10.1080/15440478.2025.2512002.

Ige, O., and H. Danso. 2021. "Physico-Mechanical and Thermal Gravimetric Analysis of Adobe Masonry Units Reinforced with Plantain Pseudo-Stem Fibres for Sustainable Construction." *Construction and Building Materials* 273:121686. https://doi.org/10.1016/j.conbuildmat.2020.121686.

ISO 22007-2. 2008. *Plastics: Determination of Thermal Conductivity and Thermal Diffusivity: Transient Plane Heat Method*. International Organization for Standardization.

Jesudass, A., V. Gayathri, R. Geethan, M. Gobirajan, and M. Venkatesh. 2021. "Earthen Blocks with Natural Fibres - A Review." *Materials Today: Proceedings* 45:6979–6986. https://doi.org/10.1016/j.matpr.2021.01.434.

Kamwa, R. A. T., J. B. Mousi, S. Tome, J. G. D. Nemaleu, M. Gérard, M.-A. Etoh, and J. Etame. 2025. "Effect of Treated Palm Fibers on the Mechanical Properties of Compressed Earth Bricks Stabilized by Alkali-Activated Binder-Based Natural Pozzolan." *International Journal of Ceramic Engineering & Science* 7 (1): e10246. https://doi.org/10.1002/ces2.10246.

Khelifi, A., M. Boumaaza, A. Belaadi, D. Tarek, A. R. G. de Azevedo, M. Bourchak, and M. Jawaid. 2024. "Effects of Alkaline Treatment of Washingtonia Mesh Waste on the Mechanical and Physical Properties of Bio-Mortar: Experimental and Prediction Models." *Biomass Conversion and Biorefinery* 14 (9): 10621–10650. https://doi.org/10.1007/s13399-023-04221-w.

Khoudja, D., B. Taallah, O. Izemmouren, S. Aggoun, O. Herihiri, and A. Guettala. 2021. "Mechanical and Thermophysical Properties of Raw Earth Bricks Incorporating Date Palm Waste." *Construction and Building Materials* 270:121824. https://doi.org/10.1016/j.conbuildmat.2020.121824.

Kooshkaki, A., and H. Eskandari-Naddaf. 2019. "Effect of Porosity on Predicting Compressive and Flexural Strength of Cement Mortar Containing Micro and Nano-Silica by Multi-Objective ANN Modeling." *Construction and Building Materials* 212:176–191. https://doi.org/10.1016/j.conbuildmat.2019.03.243.

Laborel-Préneron, A., J. E. Aubert, C. Magniont, C. Tribout, and A. Bertron. 2016. "Plant Aggregates and Fibers in Earth Construction Materials: A Review." *Construction and Building Materials* 111:719–734. https://doi.org/10.1016/j.conbuildmat.2016.02.119.

Li, L., Y. Wan, S. Chen, W. Tian, W. Long, and J. Song. 2022. "Prediction of Optimal Ranges of Mix Ratio of Self-Compacting Mortars (SCMs) Based on Response Surface Method (RSM)." *Construction and Building Materials* 319:126043. https://doi.org/10.1016/j.conbuildmat.2021.126043.

Li, X., C. M. Ho, S. I. Doh, M. I. Al Biajawi, Q. Ma, D. Zhao, and R. Liu. 2025. "Strength Characteristics and Prediction of Ternary Blended Cement Building Material Using RSM and ANN." *Buildings* 15 (5): 5. https://doi.org/10.3390/buildings15050733.

Limami, H., D. Guettioui, O. Dahi, E. Mehdi El Boustani, I. Manssouri, A. El Alami, and A. Khaldoun. 2023. "Machine Learning Forecasting of Thermal, Mechanical and Physicochemical Properties of Unfired Clay Bricks with Plastic Waste Additives." *Materials Today: Proceedings* 72:3509–3513. https://doi.org/10.1016/j.matpr.2022.08.218.

Maaze, M. R., and S. Shrivastava. 2023. "Selection of Eco-Friendly Alternative Brick for Sustainable Development; A Study on Technical, Economic, Environmental and Social Feasibility." *Construction and Building Materials* 408:133808. https://doi.org/10.1016/j.conbuildmat.2023.133808.

Mebarkia, R., M. Bouzeroura, M. Boumaaza, N. Chelouah, A. Belaadi, I. M. H. Alshaikh, Y. Chetbani, and D. Ghernaout. 2025a. "Upcycling Cement Kiln Dust for Manufacturing Clay Bricks Fired at Different Temperatures: RSM and ANN-GA Hybrid-Optimization." *Results in Engineering* 27:105683. https://doi.org/10.1016/j.rineng.2025.105683.

Mebarkia, R., M. Bouzeroura, M. Boumaaza, N. Chelouah, A. Belaadi, I. M. H. Alshaikh, Y. Chetbani, and D. Ghernaout. 2025b. "Upcycling Cement Kiln Dust for Manufacturing Clay Bricks Fired at Different Temperatures: RSM and ANN-GA Hybrid-Optimization." *Results in Engineering* 27:105683. https://doi.org/10.1016/j.rineng.2025_105683.

Medjelekh, D., L. Ulmet, S. Abdou, and F. Dubois. 2016. "A Field Study of Thermal and Hygric Inertia and Its Effects on Indoor Thermal Comfort: Characterization of Travertine Stone Envelope." *Building & Environment* 106:57–77. https://doi.org/10.1016/j.buildenv.2016.06.010.

Millogo, Y., J.-C. Morel, J.-E. Aubert, and K. Ghavami. 2014. "Experimental Analysis of Pressed Adobe Blocks Reinforced with Hibiscus Cannabinus Fibers." *Construction and Building Materials* 52:71–78. https://doi.org/10.1016/j.conbuildmat.2013.10.094.

Nakkeeran, G., L. Krishnaraj, P. Shakor, G. U. Alaneme, and O. N. Otu. 2024. "Mechanical Properties Optimization and Cost Analysis of Agricultural Waste as an Alternative in Brick Production." *Scientific Reports* 14 (1): 24075. https://doi.org/10.1038/s41598-024-74970-9.

NF EN 1015–11, A. 2000. *Méthodes D'Essai Des Mortiers Pour Maçonnerie-Partie 11: Détermination De La Résistance à La Flexion Et à La Compression Du Mortier Durci*. Technical Report.

NF EN P13-901. 2017. *Blocs De Terre Comprimée Pour Murs Et Cloisons-Définitions-Spécifications-Méthodes D'Essai-Conditions De Réception*. Saint-Denis La Plaine Ce-Dex: AFNor.

NF P 18-560. 1990. *Granulats-Analyse Granulométrique Par Tamisage*. Paris: AFNOR.

Ofuyatan, O. M., O. B. Agbawhe, D. O. Omole, C. A. Igwegbe, and J. O. Ighalo. 2022. "RSM and ANN Modelling of the Mechanical Properties of Self-Compacting Concrete with Silica Fume and Plastic Waste as Partial Constituent Replacement." *Cleaner Materials* 4:100065. https://doi.org/10.1016/j.clema.2022.100065.

Omrani, H., L. Hassini, A. Benazzouk, H. Beji, and A. Elcafsi. 2020. "Elaboration and Characterization of Clay-Sand Composite Based on Juncus acutus Fibers." *Construction and Building Materials* 238:117712. https://doi.org/10.1016/j.conbuildmat.2019.117712.

Oti, J. E., and J. M. Kinuthia. 2020. "The Development of Stabilised Clay-Hemp Building Material for Sustainability and Low Carbon Use." *Journal of Civil Engineering and Construction* 9 (4): 205–214. https://doi.org/10.32732/jcec.2020.9.4.205.

Poinot, T., M. E. Laracy, C. Aponte, H. M. Jennings, J. A. Ochsendorf, and E. A. Olivetti. 2018. "Beneficial Use of Boiler Ash in Alkali-Activated Bricks." *Resources, Conservation & Recycling* 128:1–10. https://doi.org/10.1016/j.resconrec.2017.09.013.

Rashid, K., E. U. Haq, M. S. Kamran, N. Munir, A. Shahid, and I. Hanif. 2019. "Experimental and Finite Element Analysis on Thermal Conductivity of Burnt Clay Bricks Reinforced with Fibers." *Construction and Building Materials* 221:190–199. https://doi.org/10.1016/j.conbuildmat.2019.06.055.

Salih, M. M., A. I. Osofero, and M. S. Imbabi. 2020. "Constitutive Models for Fibre Reinforced Soil Bricks." *Construction and Building Materials* 240:117806. https://doi.org/10.1016/j.conbuildmat.2019.117806.

Serebe, Y. A. A., M. Ouedraogo, A. D. Sere, I. Sanou, W.-K. J. E. Zagre, J.-E. Aubert, M. Gomina, and Y. Millogo. 2024. "Optimization of Kenaf Fiber Content for the Improvement of the Thermophysical and Mechanical Properties of Adobes." *Construction and Building Materials* 431:136469. https://doi.org/10.1016/j.conbuildmat.2024.136469.

Sinkhonde, D., R. O. Onchiri, W. O. Oyawa, and J. N. Mwero. 2021. "Response Surface Methodology-Based Optimisation of Cost and Compressive Strength of Rubberised Concrete Incorporating Burnt Clay Brick Powder." *Heliyon* 7 (12): e08565. https://doi.org/10.1016/j.heliyon.2021.e08565.

Taallah, B., and A. Guettala. 2016. "The Mechanical and Physical Properties of Compressed Earth Block Stabilized with Lime and Filled with Untreated and Alkali-Treated Date Palm Fibers." *Construction and Building Materials* 104:52–62. https://doi.org/10.1016/j.conbuildmat.2015.12.007.

Taallah, B., A. Guettala, S. Guettala, and A. Kriker. 2014. "Mechanical Properties and Hygroscopicity Behavior of Compressed Earth Block Filled by Date Palm Fibers." *Construction and Building Materials* 59:161–168. https://doi.org/10.1016/j.conbuildmat.2014.02.058.

Tan, X., J. Xing, Y. Wang, H. Qiu, S. Mahjoubi, and P. Guo. 2026. "Explainable Machine Learning for Predicting Compressive Strength of Rubberized Concrete: SHAP Interpretation, Lifecycle Assessment, and Design Recommendations." *Journal of Cleaner Production* 538:147338. https://doi.org/10.1016/j.jclepro.2025.147338.

Tran, K. Q., T. Satomi, and H. Takahashi. 2018. "Improvement of Mechanical Behavior of Cemented Soil Reinforced with Waste Cornsilk Fibers." *Construction and Building Materials* 178:204–210. https://doi.org/10.1016/j.conbuildmat.2018.05.104.

Wang, Y., A. A. AL-Huqail, S. Salimimoghadam, K. Jasim Mohammed, A. Jan, H. E. Ali, M. Amine Khadimallah, and H. Assilzadeh. 2022. "The Metaheuristic Optimization of the Mechanical Properties of Sustainable Energies Using Artificial Neural Networks and Genetic Algorithm: A Case Study by Eggshell Fine Waste." *International Journal of Energy Research* 46 (15): 21338–21352. https://doi.org/10.1002/er.8255.

Wang, Z., and A. Sobey. 2020. "A Comparative Review Between Genetic Algorithm Use in Composite Optimisation and the State-of-the-Art in Evolutionary Computation." *Composite Structures* 233:111739. https://doi.org/10.1016/j.compstruct.2019.111739.

XP P13-901. 2017. *Blocs De Terre Comprimée Pour Murs Et Cloisons-Définitions-Spécifications-Méthodes D'Essai-Conditions De Réception*. Saint-Denis La Plaine Ce-Dex: AFNor.

Zardari, M. A., N. A. Lakho, and M. A. Amur. 2020. "Structural Behaviour of Large Size Compressed Earth Blocks Stabilized with Jute Fiber." *Journal of Engineering Research* 8 (2): 60–72. https://doi.org/10.1016/S2307-1877(25)00748-5.